

INVESTIGATION OF 2-OXOACID OXIDOREDUCTASES IN *METHANOCOCCUS*
MARIPALUDIS AND LARGE-SCALE GROWTH OF *M. MARIPALUDIS*

by

BRIAN W. WATERS

(Under the direction of Dr. William B. Whitman)

ABSTRACT

With the emergence of *Methanococcus maripaludis* as a genetic model for methanogens, it becomes imperative to devise inexpensive yet effective ways to grow large numbers of cells for protein studies. Chapter 2 details methods that were used to cut costs of growing *M. maripaludis* in large scale. Also, large scale growth under different conditions was explored in order to find the conditions that yield the most cells.

Chapter 3 details the phylogenetic analysis of 2-oxoacid oxidoreductase (OR) homologs from *M. maripaludis*. ORs are enzymes that catalyze the oxidative decarboxylation of 2-oxoacids to their acyl-CoA derivatives in many prokaryotes. Also in chapter 3, a specific OR homolog in *M. maripaludis*, an indolepyruvate oxidoreductase (IOR), was mutagenized, and the mutant was characterized. PCR and Southern hybridization analysis showed gene replacement. A no-growth phenotype on media containing aromatic amino acid derivatives was found.

INDEX WORDS: *Methanococcus maripaludis*, fermentor, 2-oxoacid oxidoreductase, indolepyruvate oxidoreductase

INVESTIGATION OF 2-OXOACID OXIDOREDUCTASES IN *METHANOCOCCUS*
MARIPALUDIS AND LARGE-SCALE GROWTH OF *M. MARIPALUDIS*

by

BRIAN W. WATERS

B.S., The University of Georgia, 1999

A Thesis Submitted to the Graduate Faculty of The University of Georgia in Partial
Fulfillment of the Requirements for the Degree

MASTER OF SCIENCE

ATHENS, GEORGIA

2002

© 2002
Brian W. Waters
All Rights Reserved

INVESTIGATION OF 2-OXOACID OXIDOREDUCTASES IN *METHANOCOCCUS*
MARIPALUDIS AND LARGE-SCALE GROWTH OF *M. MARIPALUDIS*

by

BRIAN W. WATERS

Approved:

Major Professor: William B. Whitman

Committee: Lawrence Shimkets
Timothy Hoover

Electronic Version Approved:

Maureen Grasso
Dean of the Graduate School
The University of Georgia
December 2002

ACKNOWLEDGMENTS

I would like to express my sincere gratitude to my parents, Charles Cofield and Kathy Cofield and my sisters Jennifer, Wendy, Jamie and Jodi for all of their love and support they have given me during my college career. I would also like to thank my father, James Waters, for his love and support as well as all my aunts, uncles, cousins and grandparents. I would also like to thank to Dr. William B. Whitman for all of the patience and wise guidance he has provided me over my time as a student in his lab. Finally, I would like to thank all of my labmates, past and present, for their help and advice.

TABLE OF CONTENTS

	Page
ACKNOWLEDGEMENTS	iv
LIST OF TABLES	vi
LIST OF FIGURES	vii
CHAPTER	
1 INTRODUCTION AND LITERATURE REVIEW	1
2 GROWTH OF <i>METHANOCOCCUS MARIPALUDIS</i> IN LARGE SCALE ...	21
Introduction.....	22
Materials and Methods.....	22
Results.....	24
Discussion.....	28
3 INVESTIGATION OF 2-OXOACID OXIDOREDUCTASES IN <i>METHANOCOCCUS MARIPALUDIS</i> STRAIN S2	36
Introduction.....	37
Materials and Methods.....	39
Results.....	44
Discussion.....	61
REFERENCES	107

LIST OF TABLES

		Page
Chapter 3		
Table 3.1.	Primer sequences for PCR amplification of OR gene sequences and control sequences for single recombination.....	64
Table 3.2.	Primer sequences for PCR amplification of IOR gene sequences for double recombination.....	65
Table 3.3.	Annealing temperatures for primer sets.....	66
Table 3.4.	Vector information.....	67
Table 3.5.	Primers used for verification of mutant genotype	68
Table 3.6.	Transformation efficiencies in <i>M. maripaludis</i> strain S2	69
Table 3.7.	Identities of <i>iorA</i> 0451 mutants in <i>M. maripaludis</i> strain S2	70
Table 3.8.	ORF annotation and homology in <i>Methanothermobacter thermautotrophicus</i> strain ΔH	73
Table 3.9.	ORF annotation and homology in <i>Methanococcus maripaludis</i> strain S2	76
Table 3.10.	ORF annotation and homology in <i>Methanococcus voltae</i>	79
Table 3.11.	ORF annotation and homology in <i>Methanothermococcus thermolithotrophicus</i>	82
Table 3.12.	ORF annotation and homology in <i>Methanocaldococcus jannaschii</i>	85
Table 3.13.	Commonly used abbreviations.....	106

LIST OF FIGURES

	Page(s)
Chapter 2	
Figure 2.1. Growth of <i>Methanococcus maripaludis</i> in McN + sodium formate medium at pH 6.8, 7.2, 7.8, and 8.0.....	30
Figure 2.2. Modeling bicarbonate concentrations under an atmosphere of 20% and 75% CO ₂ fermentor headspace.....	32
Figure 2.3. Growth of <i>Methanococcus maripaludis</i> strain S2 in McN + 0.4 and 0.7 M sodium formate at various pHs.....	34
Chapter 3	
Figure 3.1. Putative 2-oxoacid oxidoreductase genes in <i>Methanothermobacter thermotrophicus</i> strain ΔH.....	71
Figure 3.2. Putative 2-oxoacid oxidoreductase ORFs in <i>Methanococcus maripaludis</i> strain S2.....	74
Figure 3.3. Putative 2-oxoacid oxidoreductase ORFs in <i>Methanococcus voltae</i>	77
Figure 3.4. Putative 2-oxoacid oxidoreductase ORFs in <i>Methanothermococcus thermolithotrophicus</i>	80
Figure 3.5. Putative 2-oxoacid oxidoreductase ORFs in <i>Methanocaldococcus jannaschii</i>	83
Figure 3.6. Phylogenetic analysis of oxidoreductase alpha subunit homologs.....	86
Figure 3.7. Phylogenetic analysis of oxidoreductase beta subunit homologs.....	88
Figure 3.8. Phylogenetic analysis of oxidoreductase gamma subunit homologs.....	90
Figure 3.9. Phylogenetic analysis of indolepyruvate oxidoreductase alpha subunit homologs.....	92
Figure 3.10. Phylogenetic analysis of coenzyme F ₃₉₀ synthetase homologs.....	94
Figure 3.11. Insertional mutagenesis of MM00451 by pIJA03-iorA0451D.....	96
Figure 3.12. Gel electrophoresis of wild-type and IORA 0451 mutant genomic DNA PCR products.....	98
Figure 3.13. Southern hybridization analysis of wild type and 451 IOR mutant genomic DNA.....	100
Figure 3.14. Growth of wild-type and mutant <i>Methanococcus maripaludis</i> strain S2 on McN, McN + aromatic amino acid derivatives and McC.....	102
Figure 3.15. Reversion growth experiment of wild-type and 451D #8 mutant in McN and McN + aromatic amino acid derivatives.....	104

CHAPTER 1

INTRODUCTION AND LITERATURE REVIEW

Physiology and ecology of methanogens

Methanogens are bacteria that belong in the domain Archaea (Woese *et al.*, 1990). Methanogens occupy a diverse selection of habitats, and they also occupy important niches within these habitats. The purpose of this section of the literature review is to explore the unique physiological features and habitats of methanogens.

Membrane lipid composition is one major difference between the methanogens as well as other Archaea, and the Bacteria. In Archaea, the membrane lipids consist of isoprenoid alcohols, ether-linked to glycerol. The chains of isoprenoid alcohols form monoglycerol diethers when linked to one glycerol and diglycerol tetraethers when linked to two glycerol molecules (De Rosa *et al.*, 1986). Many methanogens have both di- and tetraethers present in their membranes. In contrast, bacterial membranes are composed of diester lipids (White, 1995).

The cell wall marks the next major area of difference between methanogens and bacteria. Both gram-negative and gram-positive bacteria contain a cell wall made of murein (peptidoglycan), in which chains are formed of repeating units of N-acetylmuramic acid and N-acetylglucosamine linked together by β 1-4 linkages. Tetrapeptide bridges link the polysaccharide chains to one another to form the peptidoglycan lattice (White, 1995). Archaeal cell walls do not contain murein, although the cell walls of some methanogens contain pseudomurein, a peptidoglycan which has N-acetyltalosaminuronic acid substituted for N-acetylmuramic acid linked with N-acetylglucosamine in a β 1-3 linkage instead of a β 1-4 linkage as in murein (White, 1995). Archaeal cell walls can also be entirely protein in composition, and the protein cell wall is known as the surface or S-layer. The S-layer in members of the order

Methanococcales, also known as the methanococci, are regular hexagonal structures covering the entire cell (Jarrell and Koval, 1989). While the S-layer is not unique to methanococci, the S-layer is common to all known methanococci.

The above points illustrate a few differences between Archaea and Bacteria. It is important to note, however, that differences can exist not only between members of different domains but between members of the same domain as well. The following discussion of methanogens, in particular the methanococci, illustrates this point.

Methanogens have been found in a wide variety of environments. A sample of the environments where methanogens have been found include salt marshes (Jones *et al.*, 1984), hypersaline lakes (Cytryn *et al.*, 2000), rice fields (Lehmann-Richter *et al.*, 1999), arctic glaciers (Skidmore *et al.*, 2000) and rumen of cattle (Whitford *et al.*, 2001). Not only do methanogens live in a wide range of habitats, they also impact their environments in many ways. Methanogens negatively impact host cattle by directing carbon flow from volatile fatty acids to methane which contributes to global warming (Johnson and Johnson, 1995). With the increase in cattle in the world to meet the demands of a growing population, this is a serious concern.

Phylogeny of methanogens

As stated previously, methanogens are members of the domain Archaea. All of the domains of life (Archaea, Bacteria and Eukarya) can be differentiated by 16S rRNA sequence data. All methanogens are located in the phylum *Euryarchaeota*, and the methanogens are divided into 5 orders: *Methanobacteriales*, *Methanococcales*, *Methanomicrobiales*, *Methanosarcinales* and *Methanopyrales* (Balch *et al.*, 1979). Among members of different orders, the 16S rRNA sequence similarity is no more than

82%. For reference, if two organisms have a 16S rRNA sequence similarity of less than 98%, then those two organisms are considered to be members of different species (Goebel and Stackebrandt, 1994) and less than 93-95% similarity indicates separate genera (Devereux *et al.*, 1990).

Members of the order *Methanobacteriales* are subdivided into two families: *Methanobacteriaceae* and *Methanothermaceae*. Members of the different families have 16S rRNA sequence similarities of less than 90%. Out of the two families, *Methanobacteriaceae* has the most members, while *Methanothermaceae* has only two isolated organisms. One of the most significant differences between the two families, besides sequence data, is motility. Only the *Methanothermaceae* are motile by means of flagella.

Within the *Methanobacteriaceae*, there have been considerable changes in the nomenclature of some of the members. One of the changes is the grouping of all of the thermophilic methanobacteria into a new genus *Methanothermobacter* (Wasserfallen *et al.*, 2000). Additionally, based on 16S rRNA data, an organism once known as *Methanothermobacter thermautotrophicus* strain Marburg has been reclassified in a new species, *Methanothermobacter marburgensis* (Wasserfallen *et al.*, 2000).

The order *Methanopyrales* consists of a single member, *Methanopyrus kandleri*. The genome sequence of *M. kandleri* was recently solved (Slesarev *et al.*, 2002). The *Methanopyrales* are quite different from the other orders of methanogens. Despite being placed in the *Euryarchaeota*, *Methanopyrales* has much in common with members of *Crenarchaeota*, which is another phylum of Archaea (Burggraf *et al.*, 1991).

The order *Methanomicrobiales* is the most diverse order of the methanogens with 3 families: *Methanomicrobiaceae*, *Methanocorpusculaceae* and *Methanospirillaceae*. The *Methanomicrobiaceae* is the largest family under the order with 6 different genera. The *Methanospirillaceae* consist of one species, *Methanospirillum hungatei*, and the *Methanocorpusculaceae* consist of four members, 3 of which are *Methanocorpusculum parvum* (Zellner *et al.*, 1989), *M. bavaricum* (Zellner *et al.*, 1989) and *M. labreanum* (Zhao *et al.*, 1989).

In addition to the three previously described families under the *Methanomicrobiales*, there is another organism grouped within the order, the classification of which is unknown below the order level. *Methanocalculus halotolerans* was isolated from an oil well in Alsace, France (Ollivier *et al.*, 1998). Based on 16S sequence data, the closest relatives of *M. halotolerans* are located in the families *Methanospirillaceae* and *Methanocorpusculaceae* (Ollivier *et al.*, 1998). Since the 16S sequence data from *M. halotolerans* is equally similar to members from both of these families, the classification of the organism is uncertain.

All members of *Methanosarcinales* are either methylotrophs or acetotrophs. Methylotrophs are methanogens that produce methane from methanol and other C1 methyl compounds. Acetotrophs produce methane from acetate. While methylotrophy is not unique to the *Methanosarcinales*, acetotrophy is. One member of the *Methanosarcinales*, *Methanosarcina barkeri*, is one example of an acetotrophic methanogen. The type strain of *M. barkeri*, strain MS, was isolated from sewage sludge. *M. barkeri* and other *Methanosarcina* as well as *Methanosaeta concilii* are the only methanogens isolated thus far that are able to produce methane from acetate.

The order *Methanococcales* consists of two families: *Methanococcaceae* and *Methanocaldococcaeae*. The family *Methanococcaceae* is subdivided into two genera: *Methanococcus* and *Methanothermococcus*. The two genera that fall under the family *Methanocaldococcaeae* are *Methanocaldococcus* and *Methanotorris*. *Methanocaldococcus* is differentiated from the mesophilic *Methanococcus* and the thermophilic *Methanothermococcus* by its hyperthermophilicity. The optimal growth temperature for *Methanocaldococcus jannaschii* is 85°C, and the optimal growth temperatures for *Methanococcus maripaluidis* and *Methanothermococcus thermolithotrophicus* are 37°C and 60-65°C, respectively. *Methanocaldococcus* is differentiated from *Methanotorris* by 16S rRNA sequence as well as some phenotypic characteristics (Graham *et al.*, 2001). Additionally, even though there is a 92-93% 16S rRNA sequence similarity between *Methanocaldococcus* and *Methanotorris*, many phylogenetic treeing algorithms indicate that the two organisms should belong in different families (Boone *et al.*, 1993).

Members of the order *Methanococcales* are obligately anaerobic archaea, and they reduce CO₂ to methane using electrons from formate or hydrogen gas (Balch and Wolfe, 1979). Selenium is stimulatory to growth of most methanococci, and members of the family *Methanococcaceae* can be mesophilic or thermophilic (Balch and Wolfe, 1979).

Members of the genus *Methanococcus* are irregular cocci approximately 1.0-2.0 µm in diameter. *Methanococcus* cells are sensitive to surfactants, and they lyse readily when placed in solutions containing low concentrations of sodium dodecylsulfate (Whitman *et al.*, 1986). The pH optimum for growth is between 6 and 8, and

Methanococcus cells require an environmental NaCl concentration of 0.5%-4% to grow. Because of this salt requirement, the cells live in salt marshes and other marine environments.

Genetic systems of methanogens

For molecular studies on an organism, several things are helpful. The first is a genome sequence. The second is a system for mutagenizing genes of interest. Research in methanogens and methanogenesis only began to pick up in the 1980s, and molecular studies were underway by the 1990s. As a result, there has been little progress until recently. There are several reasons why genetic systems have developed rather slowly for methanogens. One reason is the relative difficulty in culturing methanogens (Tumbula and Whitman, 1999). Since methanogens are obligately anaerobic, culturing requires special medium preparation techniques designed to remove oxygen. Also, growth of the organisms must be done either in sealed tubes or, if grown on plates, in sealed containers. Another reason for the slow development of genetic systems is the lack of selectable markers for methanogens (Bock and Kandler, 1985). Despite these setbacks, there have been significant advances made in molecular techniques designed for methanogens. One of the largest advances in recent years has been the resolution of complete genome sequences of five methanogens.

The complete genome sequences for five methanogens: *Methanothermobacter thermautotrophicus* (Smith *et al.*, 1997), *Methanopyrus kandleri* (Slesarev *et al.*, 2002), *Methanosarcina acetivorans* (Galagan *et al.*, 2002), *Methanosarcina mazei* (Deppenmeier *et al.*, 2002) and *Methanocaldococcus jannaschii* (Bult *et al.*, 1996) are currently available. Additionally, there are several nearly complete genome sequences

including *Methanosarcina barkeri*, *Methanothermococcus thermolithotrophicus*, *Methanococcus voltae* and *Methanococcus maripaludis*, which is the organism of interest in this thesis.

Another advance made in establishing a gene transfer system for studying methanogens has been the discovery of transformation methods that work for them. One such transformation method is a polyethylene glycol-mediated transformation procedure for *Methanococcus maripaludis* (Tumbula *et al.*, 1994). Other examples include an electroporation method for *Methanococcus voltae* (Patel *et al.*, 1994). To date, no method of transduction has been refined for methanogens, although there are phages capable of infecting *M. voltae* (Wood *et al.*, 1989).

An additional requirement for a genetic system in an organism is the availability of markers for selection. Puromycin resistance has been found to work well as a marker in methanogens. Puromycin is an antibiotic which binds to the A-site in ribosomes and stops protein synthesis. The puromycin resistance cassette, or *pac* cassette, consists of a puromycin transacetylase (*pac*) gene from *Streptomyces alboniger*. A promoter and terminator from the methylreductase operon in *Methanococcus voltae* is added to allow expression of the *pac* gene in methanococci to form the complete *pac* cassette (Gernhardt *et al.*, 1990).

Vectors for genetic studies in methanogens have been under development in recent years. In particular, several shuttle vectors have been engineered for methanogens. One such vector is pDLT44, which was created by ligating sections of pURB500, a 8285-bp plasmid isolated from *M. maripaludis* strain C5, into pMEB.2 which contains the *pac*

cassette (Tumbula *et al.*, 1997). This shuttle vector has been successfully transformed into *Methanococcus maripaludis* strain JJ (Tumbula *et al.*, 1997).

Methanogenesis from H₂ and CO₂

Methanogenic bacteria obligately produce methane by a process known as methanogenesis. There are several carbon compounds that serve as substrates for methanogenesis. Substrates for methanogenesis include H₂ and CO₂, formate, methanol, methylamines and acetate. Unique cofactors found only in methanogens are required to produce methane from these substrates. In this section of the introduction, methanogenesis from H₂ and CO₂ is detailed.

Methanogenesis from H₂ and CO₂ is probably the most researched and understood of all the methanogenic pathways. Most methanogens discovered thus far use these two substrates to produce methane (Balch *et al.*, 1979). Methanogenesis from H₂ and CO₂ is an exergonic process that proceeds at a ΔG° value of -131 kJ/mol. However, in the environment, partial pressures of hydrogen are between 1 Pa and 10 Pa, so the free energy change in methanogenesis is between -20 kJ/mol to -40 kJ/mol. Since at least 50 kJ/mol is needed to drive the synthesis of ATP from ADP and inorganic phosphate (Thauer *et al.*, 1977), less than 1 mol of ATP is probably produced per mole of CH₄ produced *in vivo*. Despite this limited energy yield, methanococci have enough energy to form all their cellular carbon from CO₂ and, in the case of some methanococci, fix molecular nitrogen.

The first step in the reduction of CO₂ to CH₄ in methanogenesis involves the binding of CO₂ to methanofuran (MFR) and the reduction of the C-1 moiety to the formyl-level. The free energy change of this step is +16 kJ/mol (Keltjens and Van der

Drift, 1986), and this step is mediated by formylmethanofuran dehydrogenase (Karrasch *et al.*, 1988). The electron donor for this step is currently unknown.

After the formation of formylmethanofuran (CHO-MFR), the formyl group is transferred to another unusual cofactor discovered in methanogens but now known to be present in some bacteria as well. Tetrahydromethanopterin (H₄MPT) is a functional analog of tetrahydrofolate. H₄MPT-like tetrahydrofolate functions in the transfer and reduction of C-1 groups. The transfer of the formyl group in CHO-MFR to H₄MPT is catalyzed by N-formylmethanofuran:tetrahydromethanopterin formyltransferase (DiMarco *et al.*, 1990).

After the initial formation of CHO-MFR and the subsequent transfer of the formyl group to H₄MPT to form CHO-H₄MPT, what follows is the reduction of CHO-H₄MPT to CH₃-H₄MPT. This reduction is accomplished in 3 steps. The first step is a dehydration of CHO-H₄MPT to CH=H₄MPT. This step has a ΔG° of -4.6 kJ/mol. The second and third steps each involve reductions. The first of the two reductions is the reduction of CH=H₄MPT to CH₂=H₄MPT, and the second step is the reduction of CH₂=H₄MPT to CH₃-H₄MPT. The ΔG° values for the reductions are -5.5 kJ/mol and -17.2 kJ/mol respectively. The source of electrons for the two reductions is another cofactor discovered in methanogens but since found elsewhere. Coenzyme F₄₂₀ is a deazaflavin possessed by all cultured methanogens (Eirich *et al.*, 1978). It was discovered that F₄₂₀ is the electron donor for the reduction of methylenetetrahydromethanopterin (CH₂=H₄MPT) to methyltetrahydromethanopterin (CH₃-H₄MPT) which is mediated by N⁵, N¹⁰-methylene tetrahydromethanopterin reductase (Ma and Thauer *et al.*, 1990). The oxidized

F₄₂₀ is reduced by a membrane-associated F₄₂₀-reducing hydrogenase (Fauque *et al.*, 1984).

The final steps in methanogenesis from H₂ and CO₂ involve the transfer of the methyl group from CH₃-H₄MPT and the binding of the methyl group to coenzyme M to form methyl-coenzyme M (CH₃-CoM). The transfer of the methyl group is hypothesized to occur in two steps. The first step is the transfer of the methyl group to a corrinoid protein, and the second step is the transfer of the methyl group from the corrinoid to coenzyme M. This hypothesis was based on the accumulation of methylated corrinoid in the absence of coenzyme M (Kengen *et al.*, 1992). This series of reactions is catalyzed by the membrane-bound methyl-H₄MPT: coenzyme M methyltransferase and is coupled to the generation of a proton motive force.

The methyl group is then further reduced to methane and released in the final steps in methanogenesis. The reactions involve the participation of 3 coenzymes: CH₃-CoM, N-7-mercaptoheptanoyl threonine-O-phosphate (HS-HTP or coenzyme B) and coenzyme F₄₃₀. CH₃-CoM binds the enzyme methylreductase, which contains F₄₃₀ as a prosthetic group. HS-HTP reduces the methyl group, and the heterodisulfide (CoM-S-S-HTP) is formed along with methane (Ellerman *et al.*, 1988). The process of methane release does not require energy in the form of ATP (Ankel-Fuchs and Thauer, 1986). Methyl-coenzyme M reductase is composed of 3 subunits in equal proportions in the arrangement of $\alpha_2\beta_2\gamma_2$. The enzyme has an absorption peak at 425 nm due to the presence of coenzyme F₄₃₀ (Ellefson and Wolfe, 1981). X-ray crystallography has confirmed that there are two molecules of F₄₃₀ embedded in 30 angstrom long channels

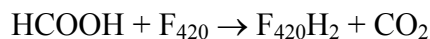
that have openings on the enzyme surface. The channels are formed by 4 subunits, which are both of the α subunits, a β and a γ subunit (Ermler *et al.*, 1997).

The proposed pathway of methane release and heterodisulfide formation involves the binding of the methyl group from $\text{CH}_3\text{-CoM}$ to the nickel center of F_{430} . The methyl group is then reduced and released as methane. Coenzyme M and HS-HTP bind to form the heterodisulfide (Ermler *et al.*, 1997). Heterodisulfide is then reduced by heterodisulfide reductase to regenerate coenzymes M and B (Hedderich *et al.*, 1990). This last step is catalyzed by a membrane-bound enzyme that couples heterodisulfide reduction with generation of a membrane potential.

Methanogenesis from formate

In addition to CO_2 , formate is a C_1 molecule that some methanogens can use as an electron donor for methanogenesis. Formate is first oxidized to CO_2 prior to the reduction to CH_4 . The difference between the two substrates is that formate does not require hydrogen and that 3 molecules of CO_2 are formed for each molecule of methane

Formate is oxidized to CO_2 by formate dehydrogenase. Formate dehydrogenase (FDH) is also found in bacteria such as *Escherichia coli* (Lester and DeMoss, 1971). In methanogens, FDH catalyzes the oxidation of formate, and this oxidation is coupled to the reduction of coenzyme F_{420} (Schauer and Ferry, 1981). The reaction proceeds as diagrammed below (Ferry, 1999):



FDH is a selenium-dependent enzyme that utilizes selenium in the form of selenocysteine (Jones *et al.*, 1979). Although activity can occur without selenium, this

results in slow growth when cells are grown on formate as a sole carbon source (Jones and Stadtman, 1981).

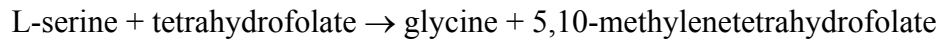
Nölling and Reeve showed that FDH is encoded by the FDH operon in *Methanobacterium thermoformicicum*, which includes the genes *fdhC*, *fdhA* and *fdhB* (Nölling and Reeve, 1997). They also showed that transcription of these genes are substrate-dependent, and there is little transcription of these genes when the cells are grown under a H₂ and CO₂ atmosphere. The same substrate-dependence of FDH activity was also shown in *Methanothermococcus thermolithotrophicus* (Sparling and Daniels, 1990).

Biosynthesis of amino acids in methanogens

Little is known about the biosynthesis of amino acids in methanogens, but results from isotope-labeling experiments have provided clues about potential pathways. In addition, the isotope-labeling experiments have provided solid data on the incorporation of carbon from substrates such as acetate and CO₂.

In *Methanothermobacter thermautotrophicus*, acetate can be assimilated and used to synthesize the amino acids alanine, aspartate and glutamate (Fuchs *et al.*, 1978). This was proven by providing ¹⁴C-labeled acetate to the cells during growth. Furthermore, the carbons in the radiolabeled acetate were incorporated into specific positions of the amino acids, with presumably reduced forms of CO₂ from methanogenesis constituting the remaining carbon. Similar specificity results were found in ¹³C-labeling experiments in *Methanospirillum hungatei* (Ekiel *et al.*, 1983). Both experiments found that the C-2 and C-3 carbons of alanine and aspartate could come from acetate, and the C-3 and C-4 carbons of glutamate could come from acetate.

Serine transhydroxymethylase was first described in methanogens in *M. thermautotrophicus* (Lin and Sparling., 1998). In bacteria and eukaryotes, this enzyme catalyzes the following reaction (Schirch, 1971):



In methanogens, tetrahydromethanopterin is used as a substrate for the reaction instead of tetrahydrofolate (Lin and Sparling, 1998). It is hypothesized that the reverse reaction is physiologically important because no known methanogen is able to use serine as a substrate for methanogenesis. Thus, this enzyme could be utilized for serine biosynthesis.

The pathway of the biosynthesis of branched-chain amino acids (BCAA), such as leucine, isoleucine and valine, has been described in methanogens. The enzymes in the pathway of BCAA biosynthesis have been characterized in *Methanococcus aeolicus*, *Methanococcus maripaludis* and *Methanococcus voltae* (Xing and Whitman, 1991). The first enzyme in the pathway is acetohydroxy acid synthase (AHAS), and it has been described for *Methanococcus aeolicus* (Xing and Whitman, 1994). AHAS requires thiamine pyrophosphate (TPP) as a prosthetic group as well as FAD for anabolic activity. In methanogens, AHAS is very sensitive to oxygen, unlike its bacterial counterpart (Xing and Whitman, 1994). Additionally, AHAS enzymes from several methanogenic archaea are sensitive to the herbicide sulfometuron methyl, like many bacterial AHASs (Xing and Whitman, 1987).

The final step in amino acid biosynthesis for many amino acids is the enzyme-mediated addition of an amino group to a keto acid analog of an enzyme. A group of enzymes called aminotransferases catalyze these reactions. Several aminotransferases

have been characterized in *Methanococcus aeolicus* (Xing and Whitman, 1992). Xing and Whitman characterized 4 different aminotransferase activities in *M. aeolicus*. These were the branched-chain aminotransferase, the aspartate aminotransferase and two aromatic amino acid aminotransferases. It was also found that 2-ketoglutarate was an inhibitor for the transamination of leucine and isoleucine. This suggests that 2-ketoglutarate may be responsible for the regulation of amino acid biosynthesis

Types of oxidoreductases

Oxidoreductases are classes of enzymes that catalyze the oxidation of one substrate coupled to the reduction of another substrate. These enzymes are involved in many diverse reactions. There are 2 main classes of oxidoreductases. They are 2-keto acid oxidoreductases and the aldehyde-oxidizing oxidoreductases. Out of these 2 main classes, this literature review will cover the 2-oxoacid oxidoreductases. There are 4 enzymes that fall under this class, and they are pyruvate oxidoreductase (POR), 2-oxoglutarate oxidoreductase (KOR), ketoisovalerate oxidoreductase (VOR) and indolepyruvate oxidoreductase (IOR). There is also an additional OR known as 2-oxoacid oxidoreductase, hereafter referred to as OFOR for 2-oxoacid:ferredoxin oxidoreductase, that has been purified and characterized from *Sulfolobus* (Zhang *et al.*, 1996)

POR is probably the most common and most studied of the oxidoreductases. The enzyme was previously known to catalyze the oxidative decarboxylation of pyruvate to acetyl-CoA, but the reaction mechanism remained speculative until the early 1970s (Uyeda and Rabinowitz, 1971). POR has been characterized from bacteria (Uyeda and Rabinowitz, 1971), archaea (Kerscher and Oesterhelt, 1981) and eukaryotes (Docampo *et*

al., 1987). POR has been purified and characterized from *Methanothermobacter thermautotrophicus* (Tersteegen *et al.*, 1997), *Methanosarcina barkeri* (Bock *et al.*, 1997) and *Methanococcus maripaludis* (Yang *et al.*, submitted). Many of the other archaea from which POR has been purified are hyperthermophilic sulfur reducers (Kletzin and Adams, 1996) or mesophilic halophiles (Kerscher and Osterhelt, 1981).

KOR is the enzyme that catalyzes the oxidative decarboxylation of 2-oxoglutarate to succinyl-CoA. It was first purified from the thermophilic archaeon *Thermococcus litoralis* (Mai and Adams, 1996). Since then, it has been purified from only one methanogen, *Methanothermobacter thermautotrophicus* (Tersteegen *et al.*, 1997).

VOR was first purified from the hyperthermophilic archaea and shown to catalyze the oxidative decarboxylation of several branched-chain 2-ketoacids (Heider *et al.*, 1996). VOR purified from *M. thermautotrophicus* was found to have the highest specific activity with 2-oxoisovalerate as a substrate (Tersteegen *et al.*, 1997).

IOR was first purified from the hyperthermophilic archaeon *Pyrococcus furiosus* (Mai and Adams, 1994). IOR was found to catalyze the oxidative decarboxylation of aromatic 2-ketoacids, such as phenylpyruvate and indole-3-pyruvate (Tersteegen *et al.*, 1997). Additionally, IORs have a large α subunit that holds most of the functional domains (Siddiqui *et al.*, 1997). This is different from other ORs, which have catalytic sites distributed over several subunits.

The OFOR from *Sulfolobus* has recently been characterized. It was found that OFOR can use pyruvate, 2-oxoglutarate and 2-oxobutyrate as substrates (Fukuda and Wakagi, 2002). This is unusual because the previously described PORs will not utilize 2-oxoglutarate, and the KORs will not utilize pyruvate.

Oxidoreductase composition

All of the 2-oxoacid oxidoreductases are multisubunit enzyme complexes. Even though the substrate specificity for each enzyme is different, all the enzymes share conserved motifs and homologous subunits. The IOR possesses the lowest number of subunits at 2, and the POR possesses the highest number of subunits at 4 (in most organisms). The VOR has 3 subunits, and the KOR has 3 as well. The KOR was found to have 4 subunits by SDS/PAGE in *M. thermautotrophicus*, but the N-terminal sequence of the extra 12 kDa subunit was not elucidated (Tersteegen *et al.*, 1997). As stated previously, all of the ORs share homologous subunits. It was found that the IOR α subunit in *Pyrococcus* sp. KOD1 shares regions of sequence similarity with the α , β and δ subunits of the PORs and IORs from other organisms (Siddiqui *et al.*, 1997). It is possible that the IOR was formed by fusion of several OR subunits in the evolutionary past. All of the ORs contain TPP-binding motifs and iron-sulfur (Fe-S) binding motifs in some of their subunits.

TPP is a prosthetic group that is found in several enzymes that catalyze decarboxylation reactions such as pyruvate dehydrogenase and pyruvate oxidoreductase (Hawkins *et al.*, 1989). TPP binds 2-oxoacids by forming a reactive carbanion, and then the carboxyl group is cleaved from the 2-oxoacid (Krampitz, 1969). TPP binds to a conserved 30-40 amino acid domain that includes a highly-conserved glycine-aspartate-glycine motif, or GDG motif (Hawkins *et al.*, 1989). With the exception of IOR, the TPP-binding motif for all 2-oxoacid oxidoreductases is found in the β subunit (Kletzin and Adams, 1996).

In the IOR α subunit, there is a putative TPP-binding motif. However, the highly conserved GDG motif is substituted with a glycine-aspartate-serine (GDS) motif (Siddiqui *et al.*, 1997). It is unclear whether this motif has the activity of a TPP-binding motif or not. However, IOR binds 2-oxoacids much like the other ORs, and this is evidence that the IOR has a functional TPP-binding motif (Tersteegen *et al.*, 1997). Additionally, TPP was found to increase the specific activity of IOR (Mai and Adams, 1994).

ORs also contain conserved cysteine residues in their δ subunits (Kletzin and Adams, 1996). The cysteines form a ferredoxin-type [4Fe-4S] motif that has the sequence CXXCXXCXXXCP (Siddiqui *et al.*, 1997; Kletzin *et al.*, 1996), where the "X" denotes any amino acid, the "C" denotes a cysteine and the "P" denotes a proline. EPR experiments performed on the pyruvate oxidoreductase purified from *Methanosarcina barkeri* have confirmed the presence of 3 4Fe-4S clusters in the POR holoenzyme (Bock *et al.*, 1997). It is hypothesized that the 4Fe-4S clusters are involved in shuttling electrons to and from the TPP prosthetic group (Charon *et al.*, 1999).

In IOR, the conserved cysteine residues are located near the carboxyl terminus of the α subunit (Siddiqui *et al.*, 1997). One difference between the conserved cysteine residues of IOR and POR is that IOR contains a putative 3Fe-4S binding motif, which has the sequence of CXXCXXCXXXXXCP (Mai and Adams, 1994; Siddiqui *et al.*, 1997). The Fe-S clusters in the δ subunit of POR contain all the 4Fe-4S clusters (Menon *et al.*, 1998).

Physiological function of 2-oxoacid oxidoreductases

The physiological roles of the 2-oxoacid oxidoreductases vary by organism. However, all of the ORs are suspected to play a role in amino acid metabolism. For many of the organisms from which ORs have been characterized thus far, the role of ORs has been in the degradation of amino acids. However, since ORs can catalyze the synthesis of 2-oxoacid precursors of amino acids from the acyl-CoAs, the possibility of the participation of ORs in amino acid synthesis cannot be discounted, although to date there have been no reported instances of ORs participating in anabolic reactions.

ORs have been hypothesized in a few hyperthermophilic archaea, such as *Pyrococcus furiosus* and *Thermococcus litoralis*, to be involved in the fermentation of amino acids to volatile fatty acids, CO₂ and H₂ (Heider *et al.*, 1996; Mai and Adams, 1994). In *P. furiosus*, the pathway for amino acid degradation first involves the deamination of amino acids to 2-oxoacids. Then, the ORs would catalyze the oxidative decarboxylation of the 2-oxoacid to an acyl-CoA derivative. Finally, the acyl-CoA would be metabolized to the volatile fatty acid, providing enough energy for ATP formation by substrate-level phosphorylation (Tersteegen *et al.*, 1997).

ORs can also be used in the biosynthesis of amino acids. *Methanothermobacter thermautotrophicus* has been hypothesized to use ORs in the synthesis of amino acids, and the pathway is hypothesized to be the opposite of that used by *P. furiosus* to ferment amino acids (Tersteegen *et al.*, 1997). It was also found that VOR from *Thermococcus litoralis* can catalyze the reductive carboxylation of isobutyryl-CoA to 2-oxoisovalerate (Heider *et al.*, 1996).

In *M. maripaludis*, it seems likely that the ORs, especially POR, catalyze the reductive carboxylation of acyl-CoAs to 2-oxoacids. *M. maripaludis* does not possess enzymes involved in the fermentation of amino acids like *P. furiosus* does, so it is unlikely that *M. maripaludis* produces energy from the fermentation of amino acids. In the case of POR, acetyl-CoA is produced by acetyl-CoA synthase (Shieh and Whitman, 1988), and the acetyl-CoA produced is used as a substrate for the POR reaction.

CHAPTER 2

GROWTH OF *METHANOCOCCUS MARIPALUDIS* IN LARGE SCALE

Introduction

To perform biochemical studies on many organisms, a large number of cells are needed to obtain sufficient cell material for study. Fermentors are capable of growing many types of cells anaerobically and aerobically in large culture volumes. Methanogens are among the organisms that can be grown in fermentors. However, little work has been done to find the optimal growth conditions of methanogens in fermentors.

Mukhopadhyay and coworkers discovered that selenium was necessary for growth of *Methanocaldococcus jannaschii*, and selenium metal was also supplied as a contaminant in the sulfide (Mukhopadhyay *et al.*, 1999). They were able to increase the final cell yield from 0.5 to 7.5 g wet cell weight/liter of culture.

M. maripaludis is regarded by some as a genetic model for methanogens. For this reason, it would be beneficial to explore methods for growing large amounts of cells so that biochemical studies may be conducted. For this study, *M. maripaludis* was grown in a 16 L fermentor. Various aspects of fermentor growth were explored such as pH optimum and CO₂ concentration. In this preliminary study, the optimal growth conditions of *M. maripaludis* were explored in a medium that contained formate as the sole carbon and energy source.

Materials and Methods

Small scale media, growth and culture conditions

M. maripaludis strain JJ was grown in McN medium. McN was prepared by adding (per 100 ml of media): 50 ml glass distilled water and 50 ml of a general salts solution containing 0.67 g/L KCl, 5.5 g/L MgCl₂ • 6 H₂O, 6.9 g/L MgSO₄ • 7 H₂O, 1 g/L NH₄Cl and 0.28 g/L CaCl₂ • 2 H₂O. A 14 g/L K₂HPO₄ solution, 1 ml, was also added

along with 1ml of a trace mineral solution which contained Na_2SeO_3 added (Whitman *et al.*, 1986). An amount of 0.5 ml of a solution of 0.2 g $\text{Fe}(\text{NH}_4)_2(\text{SO}_4)_2 \cdot 6 \text{H}_2\text{O}$ per 100 ml glass-distilled water was added, and 0.1 ml of a 1 g/100 ml solution of rezasurin was used as a redox indicator. A solution of NaCl, 7.5 ml of a 293 g/L, was added as well as 0.5 g NaHCO_3 . The medium was boiled under $\text{N}_2:\text{CO}_2$ (70:30) to remove dissolved oxygen. After boiling, 0.05 g cysteine-HCl /100 ml medium was added as a reductant. The medium was dispensed in an anaerobic chamber (Coy) into Balch tubes to a volume of 5 ml/tube. The tubes were flushed with $\text{H}_2:\text{CO}_2$ prior to sterilization.

Prior to inoculation, 1 part in 50 of a 2.5% solution of $\text{Na}_2\text{S} \cdot 9\text{H}_2\text{O}$ was added to the McN. The tubes were then inoculated with 0.2ml culture. The tubes were pressurized with $\text{H}_2:\text{CO}_2$ (80:20) to 40psi, and the cells were grown at 37°C overnight with shaking at 50 rpm.

The 5 ml cultures were transferred to 150 ml of McN. McN, 150 ml, with 0.2 g NaHCO_3 /100ml media instead of 0.5 g was dispensed into 1 L modified Wheaton bottles in an anaerobic chamber and flushed with $\text{H}_2:\text{CO}_2$ prior to sterilization. Two ml of a 2.5% solution of $\text{Na}_2\text{S} \cdot 9\text{H}_2\text{O}$ was added to the bottles prior to inoculation. The cultures were grown at 37°C overnight with shaking at 50 rpm.

Large scale growth and harvesting of *Methanococcus maripaludis*

Cells were grown in 16 L volume in a 20 L fermentor (W.B.Moore, Easton, PA). McN + 0.4 or 0.7 M sodium formate was prepared in the fermentor, and the media was sterilized. After sterilization, 16ml of 20% $\text{Na}_2\text{S} \cdot 9\text{H}_2\text{O}$ was added as a reductant. In all cases, 5 bottles containing 150 ml each of *M. maripaludis* culture grown previously was added as inoculum. The cells were grown at 200 rpm stirring under an atmosphere of N_2

and CO₂ (80% and 20%, respectively). Due to the changes in medium pH during growth, a means of pH control was needed. Formic acid, 50% v/v, was added to maintain the pH at a predetermined level. Medium pH was monitored using a fermentor pH probe (Broadley-James, Irvine, CA), and pH readings were compiled and analyzed in the fermentor's computer. Formic acid was added directly to the medium by a Masterflex C/L peristaltic pump (Barnant, Barrington, IL) which was activated by the fermentor's computer when the medium pH rose above the predetermined pH value. The pump speed was set to the lowest setting, and pH control added formic acid to the medium whenever the pH rose about 0.02 units past the preset value.

The cells were harvested with an Alfa Laval Sharples continuous-flow centrifuge at 32,000 rpm. Collected wet cell paste was placed in a serum bottle, and the bottle was stoppered, flushed and pressurized to 10 psi with H₂:CO₂ (80:20) gas mix. The cells were then stored at -20°C.

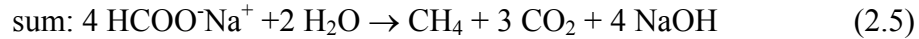
Results

Determination of pH optimum of *M. maripaludis* during large-scale growth

The pH optimum of *M. maripaludis* during large scale growth was determined. Since, as the cells grow and replicate, the medium pH becomes more alkaline, 50% formic acid was added to control the pH. In Figure 2.1, cells were cultured in the fermentor on formate at pHs 6.8, 7.2, 7.8 or 8.0. At pH 6.8, no cell growth was apparent. In contrast, *M. maripaludis* grows well at a pH of 6.8 on H₂ + CO₂ (data not shown). pH 7.8 shows the highest growth rate and cell yield.

Bicarbonate/CO₂ modeling

While growing with formate as a sole carbon and energy source, the medium that *M. maripaludis* is growing in undergoes changes in bicarbonate and formate concentrations. These changes can be expressed by the following three equations:



In equation 2.2, 4 moles of sodium formate in the medium are consumed in methanogenesis to yield 1 mole of methane. Three moles of sodium bicarbonate and 1 mole of sodium hydroxide are produced in the reaction. The mole of sodium hydroxide produced causes the medium pH to rise. This equation explains the observation that as cell number increases during growth on formate, the pH rises as well. Equations 2.3 and 2.4 diagram the conversion of sodium bicarbonate to carbon dioxide. This is a spontaneous reaction whose direction is dependent on the concentration of CO₂ within the medium and headspace as well as the pH of the medium. Equation 2.3 shows the intermediate reaction that shows the rapid formation of a mole of sodium hydroxide from 1 mole of bicarbonate. In equation 2.4, 1 mole of carbon dioxide is produced from the carbonic acid. The carbon dioxide is dissolved in the medium and then released into the headspace.

Equation 2.5 is a summary of equations 2.2, 2.3 and 2.4. Four moles of bicarbonate are required to form one mole of CH₄. The same stoichiometry of 4 mole

formate/ mole methane ratio is found in other methanogens that produce methane from formate by means of formate dehydrogenase such as *Methanobacterium formicicum* (Wu *et al.*, 1992). Missing from the summary equation is sodium bicarbonate, and this is because sodium bicarbonate undergoes spontaneous reactions to form carbonic acid and NaOH. The carbonic acid then undergoes another reaction to form CO₂.

In all fermentor runs, the initial headspace concentration of CO₂ is 20% because the vessel is flushed with that percentage CO₂. It is assumed that the CO₂ concentration will rise to 75% in the later stages of growth due to Equations 2.2 and 2.3. It is possible to calculate the molar concentration of bicarbonate in the medium by the equation below:

$$\log[\text{HCO}_3^-] = \text{pH} - \text{pK}' + \log[\text{CO}_2] \quad (2.6)$$

Equation 2.6 is a means of calculating bicarbonate concentration based on the medium pH and the concentration of CO₂. Equation 2.6 was used to calculate the bicarbonate concentration in the medium at different pHs.

Figure 2.2 shows the calculated concentrations of bicarbonate expected at different medium pHs and at equilibrium with atmospheres of 20% and 75% CO₂. Also, the beginning (20% CO₂) bicarbonate concentration was subtracted from the final (75% CO₂) bicarbonate concentration to give the expected change in bicarbonate concentration throughout the fermentor run. It was found that at pH values below 8, the increase in the bicarbonate concentration remained lower than 0.5 M. This is an important point because at higher pH, more bicarbonate is produced as the net reaction is pulled in that direction. Bicarbonate is produced as CO₂ is pulled from the vessel headspace into the medium, and upon reaction with water, the CO₂ forms carbonate which releases a proton to form bicarbonate. The proton neutralizes the NaOH. Because of this, less formic acid is added

to the medium to neutralize NaOH formed upon sodium formate oxidation. Therefore, if the concentration of formate in the medium is not greater than the increase in the concentration of bicarbonate, then the cells will starve when the formate is depleted. pH values lower than 7.0 or higher than 8.0 are outside the growth range for *M. maripaludis*, so growth will not occur due to reasons other than the change in bicarbonate concentration. Nevertheless, the results suggest that lower formate concentrations can be used, and a lower formate concentration was tested to see if it could yield similar results to higher concentrations.

Growth of *M. maripaludis* on lowered formate medium concentrations

Previously, a medium formate concentration of 0.7 M was used to grow *M. maripaludis*. Since formate is the most expensive part of the medium, a lower formate concentration of 0.4 M was tested so that the cost of producing *M. maripaludis* cells could be reduced.

Figure 2.3 shows the results of growth experiments using 0.4 M and 0.7 M sodium formate at various pH values. The two 0.4 M formate growth curves show growth rates and yields comparable to the two 0.7 M formate growth curves. The extended lag phase of 0.4 M formate, pH 7.5 curve may be due to variables unrelated to the pH or the formate concentration because higher growth rates were observed at the same formate concentration and pH in other experiments (data not shown). The 0.4 M formate, pH 7.2 growth curve shows growth rates similar to that of the 0.7 M formate, pH 7.8 growth curve.

Discussion

From the results of the pH and formate concentration experiments, a standard protocol for growing *M. maripaludis* in minimal medium + formate was devised. The protocol takes into account the pH changes that occur during growth as well as the cost of preparing the medium. The standard protocol was created to grow *M. maripaludis* cells cheaply and quickly.

The pH for growth was set at 7.5 for the standard protocol. Even though results showed that pH 7.8 appeared to give the best growth, pH 7.5 was selected because that pH was a "middle point" between pH 7.8 and pH 7.2. The reason why such a "middle point" is necessary is because pH control is imprecise. Since the pH of the medium is constantly rising during growth, the pH control does not keep the pH steady.

The medium formate concentration for the standard protocol was set at 0.4 M sodium formate. Growth results showed that a 0.4 M formate concentration yielded comparable growth yields to 0.7 M formate medium concentrations. This result was predicted by bicarbonate modeling.

Bicarbonate modeling predicts that even lower concentrations of formate may be used at pH 7.5. The limit set by bicarbonate modeling at pH 7.5 is 0.15 - 0.2 M formate, but these concentrations were not tested due to the expense of preparing fermentation runs. However, higher pHs will cause an increased production of bicarbonate. Protons released during bicarbonate formation will neutralize the NaOH formed during the oxidation of sodium formate. This will cause a decrease in the amount of formic acid added, and the formate in the medium will not be replenished, lowering cell yields.

Typically, 1.6 g wet cell weight/L of culture are harvested after growth of *M. maripaludis* on formate. In some experiments (data not shown), the medium concentration of selenium was increased. However, this did not increase cell yield (data not shown).

Figure 2.1: Growth of *Methanococcus maripaludis* in McN + sodium formate at pH 6.8, 7.2, 7.8, and 8.0.

Cells were grown in 16 L McN + 0.7 M sodium formate at pH 6.8, 7.2 and 7.8 (at pH 8.0, the cells were grown in 0.4 M sodium formate) until growth appeared to stop. All cultures were grown at 37°C with stirring. Immediately after inoculation, the cultures were sparged with N₂:CO₂ (80:20) for 1 minute. The pH was controlled by the addition of 50% (v/v) formic acid. The absorbance was read by collecting a small amount of medium from the fermentor and immediately reading the absorbance at 600 nm

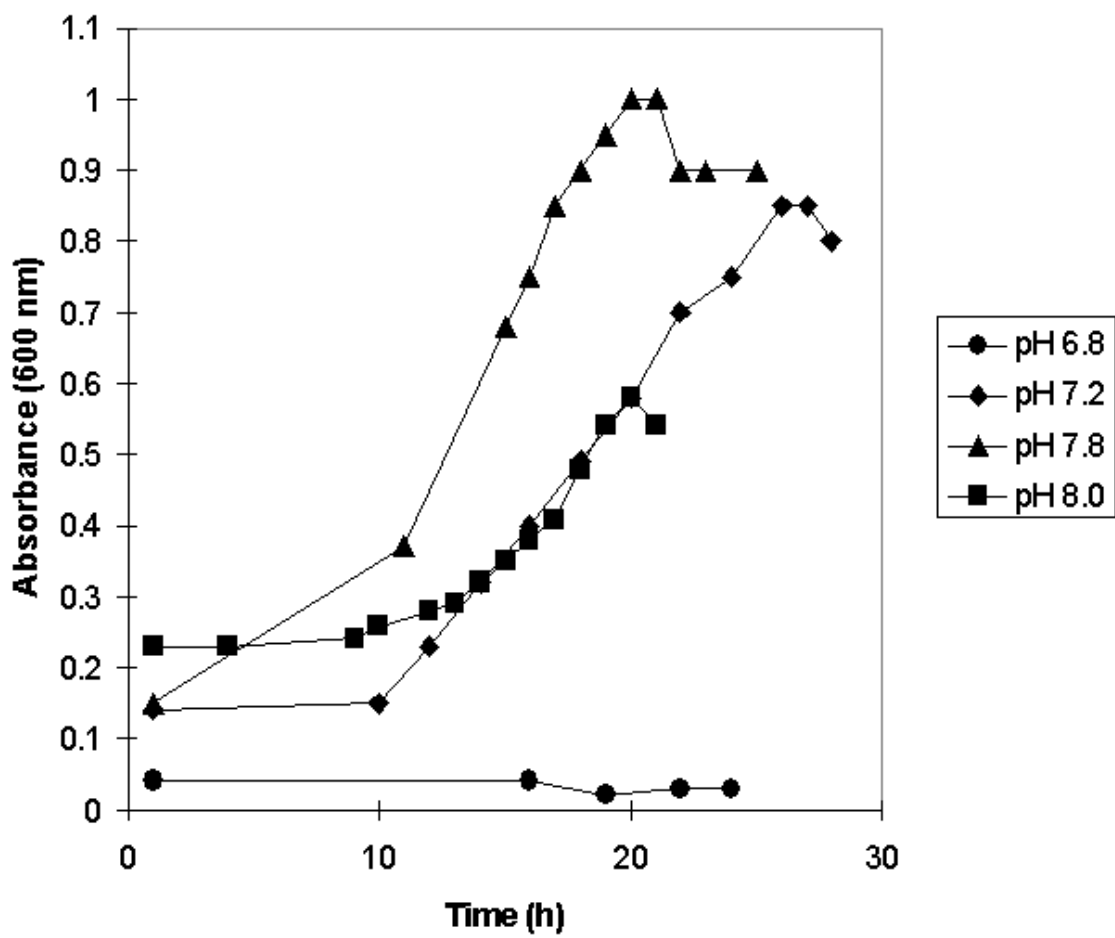


Figure 2.2: Modeling bicarbonate concentrations under an atmosphere of 20% and 75% CO₂

Theoretical concentrations of bicarbonate were calculated at a series of pHs under atmospheres of 20% and 75% CO₂. The lower concentration of CO₂ (20%) was the initial concentration before growth while 75% is the expected concentration in the logarithmic growth phase. The bicarbonate concentrations were calculated using equation 2.6. The inset graph shows the increase in medium bicarbonate concentration from pH 6 to 9, and the larger graph shows the increase in bicarbonate from pH 6 to 8. The graphs were used as a guide to determine the minimum concentration of sodium formate required to support growth at various pH values.

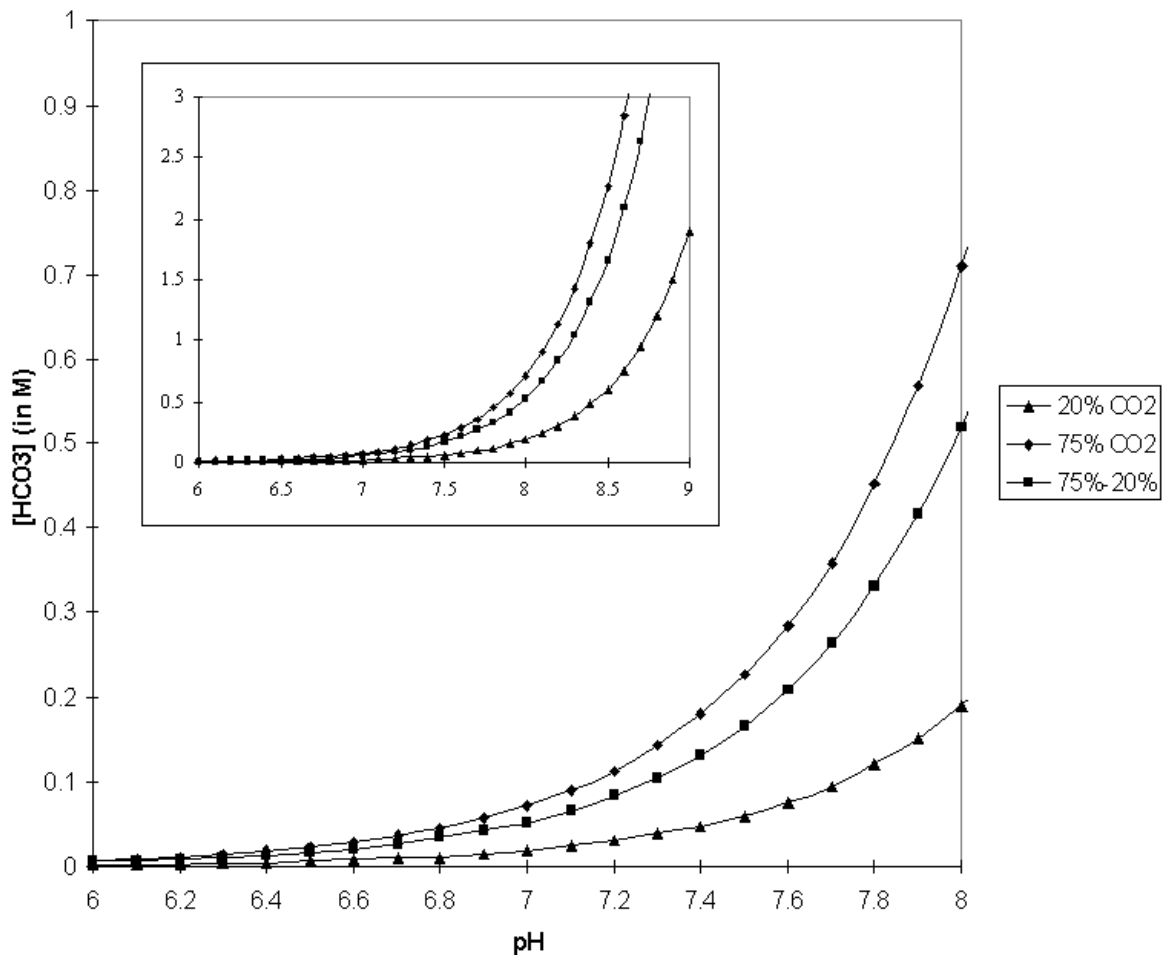
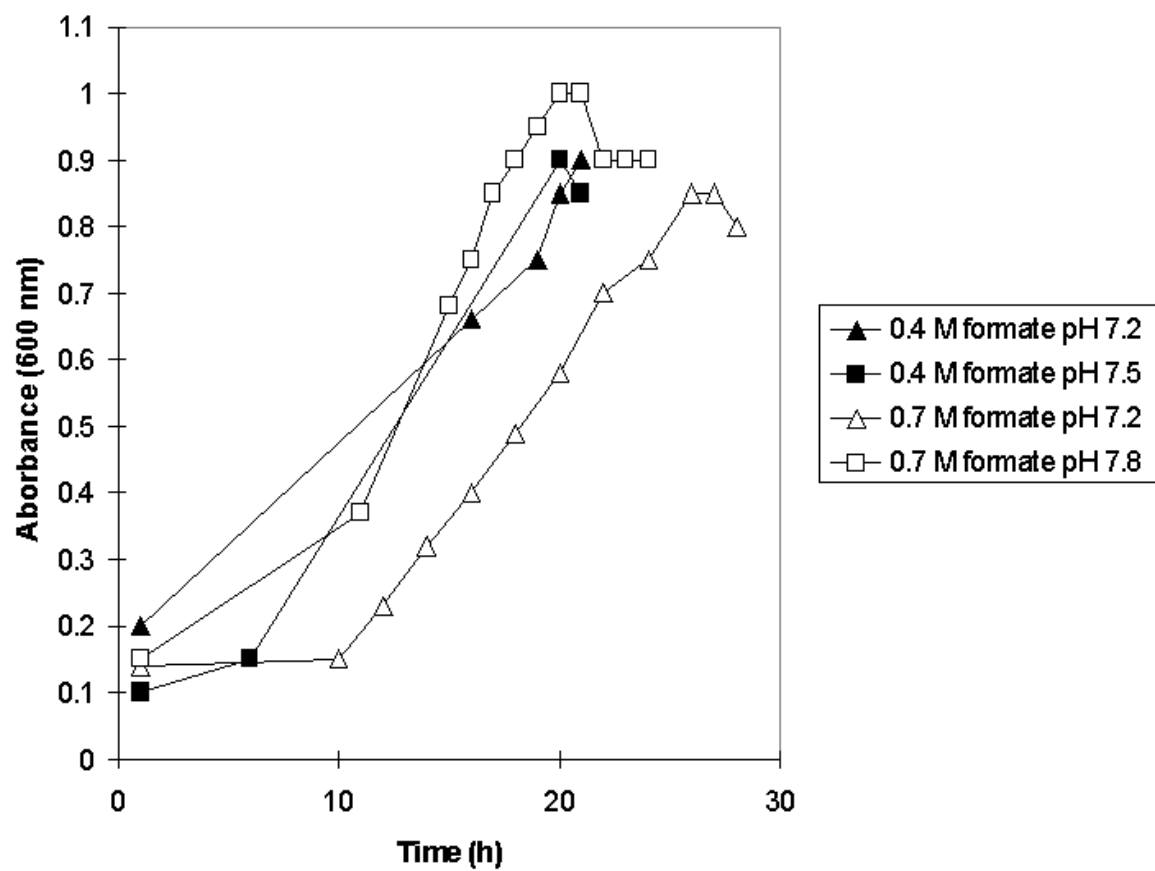


Figure 2.3: Growth of *Methanococcus maripaludis* strain S2 in McN + 0.4 M and 0.7 M sodium formate at various pHs

Cells were grown in 16 L McN + 0.7 M sodium formate or McN + 0.4 M sodium formate at various pH values until growth appeared to stop. All cultures were grown at 37°C with stirring. Immediately after inoculation, the cultures were sparged with N₂:CO₂ (80:20) for 1 minute. The pH was controlled by the addition of 50% (v/v) formic acid. The absorbance of the cultures was read by collecting a small amount of medium from the fermentor and immediately reading the absorbance at 600 nm.



CHAPTER 3

INVESTIGATION OF 2-OXOACID OXIDOREDUCTASES IN *METHANOCOCCUS*

MARIPALUDIS STRAIN S2

Introduction

The role of oxidoreductase enzymes in *Methanococcus maripaludis* has not been well-studied. Two-oxoacid oxidoreductases play a role in peptide fermentation for some hyperthermophilic archaea. To date, only POR has been purified and characterized from *M. maripaludis* (Yang *et al.*, submitted). The existences of an IOR, VOR and KOR are predicted in *M. maripaludis* by phylogenetic analysis.

Phylogenetic analysis of protein sequences from organisms has proven to be a valuable predictor of protein function. Technological advances have made possible databases of genome sequences and rapid, automated sequencing methods. As a result, it is possible to conduct phylogenetic analyses over a broad range of organisms. In addition to searching for single sequences in databases, it is also possible to search for closely-related sequences, or homologs, using the FASTA (Lipman and Pearson, 1985) or the BLAST tools (Altschul *et al.*, 1990). The sequences retrieved with the FASTA or BLAST tools can be aligned by using CLUSTALW or PileUp. From the sequence alignments, meaningful evolutionary relationships can be discerned, and the information can be processed and displayed using tree-building algorithms such as Fitch-Margoliash and Neighbor-Joining, to name a few of the distance-based methods.

Although phylogenetic studies will not reveal *in vivo* protein function, the information gained from phylogenetic relationships proves to be an excellent way to predict function of unknown proteins. Sequence data is supplemented by molecular studies in which one attempts to mutagenize the gene of interest and detect changes in genotype and phenotype. Molecular studies utilize genetic tools such as knockout

vectors in which a portion of the gene of interest is ligated next to a selectable marker. The reengineered vector is then capable of integration into a target organism's genome by homologous recombination. This makes it possible to inactivate nearly any non-essential gene.

In *Methanococcus maripaludis*, there are several uncharacterized open reading frames (ORFs) that bear sequence similarity to genes that encode for 2-oxoacid oxidoreductase subunits. Part of this chapter is concerned with the phylogenetic analysis of 5 gene clusters that bear homology to characterized ORs other than POR. Those include the two gene clusters that are homologous to IOR-encoding genes; MM00451-MM00452 and MM00123-MM00122. A gene cluster that is homologous to VOR-encoding genes is MM01350-MM01348. The genes homologous to KOR-encoding genes are found at two different loci, MM00642 and MM01396-1395. The gene cluster that is homologous to a gene that encodes an unspecific OR in *Sulfolobus* is MM00112-MM00111. This preliminary study also allows us to test the hypothesis on the predicted functions of the OR homologs.

To study the role of ORs in amino acid biosynthesis, OR-encoding genes were identified by phylogenetic analysis. The genes were mutagenized by the homologous recombination of a shuttle vector, pIJA03, which contained regions of the ORs. The two IOR α homologs, MM00451 and MM00123, were selected for further study.

IOR is a 2-oxoacid oxidoreductase capable of catalyzing the reversible oxidative decarboxylation of carboxylic acids which have aromatic rings. Some of the sample substrates for the catabolic activity of IOR include phenylpyruvate and indole-3-acetate. IOR catalyzes the oxidative decarboxylation of these substrates to acyl-CoA derivatives.

It is thought that in *M. maripaludis* the reverse, anabolic reaction, or the reductive carboxylation of an acyl-CoA to a 2-oxoacid, is physiological.

To find the role of IOR in *M. maripaludis*, growth experiments were done to see if there was a specific phenotype associated with inactivation of the genes encoding this putative IOR. Mutants were grown in minimal medium, complex medium or medium with the carboxylic acid precursors of aromatic amino acids.

Materials and Methods

Phylogenetic analysis of OR homologs

The N-terminal sequences of the POR, VOR, KOR and IOR subunits obtained from *Methanothermobacter marburgensis* from Tersteegen et. al, (1997) were used to search the ERGO database (Integrated Genomics) for the complete sequences from the related species, *Methanothermobacter thermautotrophicus*. These complete oxidoreductase subunit sequences were then used to search for homologs in *Methanococcus maripaludis*, *Methanococcus voltae*, *Methanothermococcus thermolithotrophicus* and *Methanocaldococcus jannaschi* genomic sequences. The amino acid sequences of all the oxidoreductase subunit homologs were aligned using the PILEUP program on GCG (Wisconsin Genetics Group).

Phylogenetic trees were made from the aligned sequences of OR subunit homologs. Two different alignments were constructed for analysis of each of the homolog sets. A conserved sequence alignment was constructed using the region of highest sequence similarity among the protein sequences. A complete sequence alignment was constructed based on the entire amino acid sequence. In this alignment, only the regions that could not be aligned were removed. Phylogenetic analyses were

performed on both alignments using the Fitch:Margoliash algorithm and the Neighbor-joining algorithm of the PHYLIP 3.572 package (Joseph Felsenstein, University of Washington). Bootstrap values and evolutionary distances were also calculated for each tree.

PCR amplification of OR gene sequences for single recombination

Primers specific to the OR genes were constructed by Integrated DNA Technologies. Primers were also made specific to regions within the *hdrA* and *cysS*, which encode for heterodisulfide reductase (*hdrA*) and cystenyl-tRNA synthase (*cysS*) respectively. *hdrA* was used as a negative control, and *cysS* was used as a positive control for some of the transformations. The sequences of the forward and reverse primers used for amplification of parts of the ORFs are shown in the table below. In Table 3.1, the “C(6)” is referring to 6 C bases, and the restriction sites are underlined. With the exception of the primers specific to regions on MM01348, a *Bgl*III restriction site was added to the 5' end of the forward primer and an *Xba*I restriction site was added to the 5' end of the reverse primer. For MM01348, the *Bgl*III site was replaced with a *Kpn*I site. The *Xba*I site was replaced with an *Nhe*I site. This was done because there were no suitable sites for primers in MM01349, which is upstream of MM01348. *Nhe*I and *Kpn*I both have restriction sites in the second multi-cloning site (MCS) of pIJA03, which is downstream of the first MCS, which contains the *Bgl*III and *Xba*I restriction sites. The vectors constructed here were to be later modified to be suitable for use in double recombination experiments. Therefore, *Nhe*I and *Kpn*I sites were added to the primers of MM01348 in anticipation of selecting another pair of primers upstream to which *Bgl*III and *Xba*I sites could be added.

For MM00451 and MM00123, an additional set of primers was made for double recombinations. The 2nd sequence of the primers is listed in the table below. In Table 3.1, the “C(6)” is referring to 6 C bases, and the restriction sites are underlined. *KpnI* restriction sites were added to the forward primers listed in the table above, and *NheI* sites were added to the reverse primers. The names of the primers were D451FO and D451RE for the forward and reverse primers amplifying a region of MM00451, respectively. D123FO and D123RE were the forward and reverse primers amplifying a region of MM00123, respectively.

All primers were used to PCR-amplify OR gene segments. For all primer sets, the extension time was set at 1 minute for 30 cycles. Ready-To-Go PCR beads (Amersham Pharmacia Biotech) were used for all PCR reactions. Annealing temperatures for the primer sets are listed in the table below. For the primers D451FO-D451RE, which are listed in Table 3.2, the annealing temperature was set at 52°C. For D123FO-D123RE, which are also listed in table 3.2, the annealing temperature was set at 51°C. After PCR, amplification was verified by gel electrophoresis on a 0.8% agarose gel.

Construction of vectors for transformation by single recombination and cloning

PCR-amplified fragments of MM00451, MM00123 and MM00112 were digested with *BglII* and *XbaI*. The MM01348 fragment was digested with *KpnI* and *NheI*. The fragments were gel-purified using a Qiagen gel extraction kit and ligated using T4 DNA ligase (Promega) into pIJA03 that was previously digested with the same restriction endonucleases and gel-purified. The temperature for the ligation was set at 4°C overnight. After ligation, the samples were dialyzed using drop dialysis filters for 2 hours. All vectors were transformed into TOP10F' -Tet_R strains of *Escherichia coli* by

electroporation. The resistance for the electroporation was set at 200 Ω and the current was set at 2.5 V. Insertion was confirmed by gel electrophoresis, and information about the engineered vectors is listed in the table below. In the engineered vectors, “pIJA03” refers to the original plasmid that the vectors were modified from. The “iorA”, “vorA”, “unk”, “cysS” and “hdrA” refer to annotations of the ORFs that the vectors were designed to mutagenize. The “unk” tag refers to an unknown OR type. The numbers after the annotation tags identify ORFs on the ERGO database. A “D” after the end of the plasmid name means that the vector is designed for double insertion mutagenesis, so there are two regions within the plasmid homologous to regions on the OR in question as opposed to one region for single insertion mutagenesis.

Transformation into *M. maripaludis* and confirmation of genotype

The plasmids pIJA03-iorA0451, pIJA03-iorA0123, pIJA03-vorA1348 and pIJA03-unk0112 as well as the two control plasmids pIJA03-cysS0061 and pIJA03-hdrA1849 were transformed into *Methanococcus maripaludis* strain S2 by the polyethylene glycol method (Tumbula *et al.*, 1994). Later, the plasmids pIJA03-iorA0451D and pIJA03-iorA0123D were used in a separate transformation. The transformed cultures were inoculated on plates of McN + acetate, 0.2% yeast extract, 0.2% Casamino acids, vitamins and puromycin. The cells were grown under anaerobic conditions at 37°C under 25 psi of H₂:CO₂ (80:20).

The genotypes of cultures transformed with pIJA03-iorA0451D and pIJA03-iorA0123D were confirmed by PCR and Southern hybridization. A primer specific to the 5' region of the upstream cloned DNA fragments and a primer specific to the 3' end of the *pac* cassette were used to screen the mutants. The primer sequences are listed in the table

below. The primer “check-Pur1” was as the reverse primer for screening both the IOR 0123 and IOR 0451 transformants.

Southern hybridization of DIG-labeled probes to wild-type and mutant S2 genomic DNA

A Southern hybridization was performed to verify the genotype of the MM00451 mutants. A DIG High Prime DNA Labeling and Detection Starter Kit I (Roche Molecular Biochemicals) was used for all parts of the experiment. A probe was created by PCR to be specific to the 5' region of the ORF 451. The primers used to create the probe are the same as those listed in table 3.1 for MM00451. The probe was digoxigenin-labeled overnight at 37°C using Klenow fragment. Wild-type and mutant genomic DNA was digested with *EcoRV* for 3 hours at 37°C. pIJA03-iorA0451D was digested with *PvuII* and *NheI* at 37°C for 3 hrs. All 5 digested mutants, the wild-type genomic DNA and pIJA03-iorA0451 were run on a 1% agarose gel. The DNA was then transferred to a nylon membrane. DNA was fixed to the membrane by UV-crosslinking. Probes were hybridized to the membrane at 65°C overnight. Then membrane was washed in a solution containing anti-digoxigenin (DIG) antibodies, and binding was visualized by adding a color-substrate solution included in the kit.

Growth experiments with MM00451 mutants and wild-type *Methanococcus maripaludis*

Mutants of MM00451 were subjected to growth experiments. MM00451 mutants and wild-type cells were grown in 5 ml of McN, McC and McN with 5mM concentrations of p-hydroxyphenylacetate, indole-3-acetate and phenylacetate. The McN + aromatic acids medium was made by adding 10X solutions of the aromatic acids to the medium after sterilization. The 10X stocks were made by adding the solid aromatic acids to water and adding concentrated NaOH until the solids dissolved. The aromatic acid

solutions were sparged for 1 h with N₂ gas, and the sparged solutions were filter sterilized in an anaerobic chamber (Coy). All tubes were inoculated with 0.2 ml of *M. maripaludis* culture that was at the middle-log growth phase (0.5 OD at 600 nm). The wild-type and mutant strains were grown in McC prior to inoculation for the growth experiment, and the cells were centrifuged at 650 x g for 10 minutes and washed twice with McN medium before inoculation. The tubes were repressurized with a H₂:CO₂ (80:20) gas mixture every 6-8 hours during growth.

Reversion back to a wild-type phenotype in the mutants was detected by another growth experiment. Mutant cells that showed delayed growth kinetics were reinoculated into McN + 5 mM p-hydroxyphenylacetate, 5 mM indole-3-acetate and 5 mM phenylacetate. Wild-type cells grown in the same medium were used as a control.

Results

Description of *Methanothermobacter thermautotrophicus* OR homologs

As seen in Figure 3.1, strain ΔH possesses one POR, IOR, VOR and KOR. In *Methanothermobacter marburgensis*, the N-terminal sequences of all the subunits of a POR, IOR, VOR and KOR were resolved (Tersteegen *et al.*, 1997). However, the sequence of the genes from this species is not known. Therefore the N-terminal sequences were used to search the genomic sequence of the closely related species in ERGO. Matches were found in the database for all of the N-terminal sequences in the genomic sequence of strain *Methanothermobacter thermautotrophicus* strain ΔH ORFs. The matches were almost perfect, so the strain ΔH 2-oxoacid oxidoreductase genes can be assigned functions with a high reliability.

The POR α subunit in strain ΔH , MTH1739, was used as the basis for all of the POR α subunit homolog searches. Homologs were found in other organisms based on sequence similarity to MTH1739. The same was done for MTH1738, which encodes for the POR β subunit. The collected homologs were later aligned and a phylogenetic analysis was performed. Both MTH1739 and MTH1738 were used in the searches for homologs in other methanogens because the two genes bear a function assigned by previous work (Tersteegen *et al.*, 1997).

MTH1740, the POR γ subunit, is larger (~90 bp) than the POR γ subunit homologs of other organisms studied in this thesis. The POR γ subunit in strain ΔH also has 2 ferredoxin-like Fe-S binding motifs at the C-terminal. Fe-S binding motifs are not found in the other POR γ subunit homologs, but Fe-S binding motifs are found in POR δ subunit homologs. It is likely that the strain ΔH POR γ subunit is a fusion of POR γ and POR δ subunits.

MTH1852 is the ORF that encodes for the α subunit of IOR in strain ΔH . MTH1852 has 2 ferredoxin-like Fe-S binding motifs like other IOR α homologs. Also, like the other IOR α subunit homologs discussed in this thesis, the MTH1852 lacks a TPP-binding motif. This is not unexpected because hyperthermophiles other than *M. thermautotrophicus*, such as *Pyrococcus* sp. KOD1, have regions which bear only partial similarity to TPP-binding sites (Siddiqui *et al.*, 1997). In KOD1, the conserved GDG motif that is found at the N-terminal ends of TPP-binding site motifs is not present. Instead, there is a similar motif of GDS. In this regard, the MTH1852 ORF is similar to the KOD1 gene. MTH1852 has a glycine-aspartate-serine, and like KOD1 the sequences of the 40 amino acids downstream of the G-D-S motif, which are a less conserved part of

the TPP-binding site motif, are also similar. One can only speculate if the glycine-aspartate-serine motifs found in all of the IOR α subunit homologs discussed in this thesis are actually part of a TTP-binding site motif.

It is important to note that the numbers given to the ORFs from *Methanothermobacter thermautotrophicus* strain Δ H are not the numbers assigned to the ORFs in ERGO, a database maintained by Integrated Genomics from which the sequences used in this thesis were obtained. The numbers used in this thesis were assigned when the genome sequence for strain Δ H was completed (Smith *et al.*, 1997).

Description of *M. maripaludis* OR homologs

M. maripaludis strain S2 possesses 7 clusters of ORFs that each contain genes homologous to the genes encoding the subunits of 2-oxoacid:ferredoxin oxidoreductases. As seen in Figure 3.2, strain S2 contains homologs to indolepyruvate oxidoreductase (IOR), pyruvate oxidoreductase (POR), 2-oxoglutarate oxidoreductase (KOR) and 2-oxoisovalerate oxidoreductase (VOR).

Strain S2 has 2 gene clusters that have ORFs which are homologous to components of IOR. IORs possess 2 subunits. The two subunits are the large (>67 kDa) α subunit and the smaller (~15 kDa) β subunit. The same composition is seen for the two IOR homologs in S2. The large α subunit of IOR contains 2 ferredoxin-like Fe-S cluster motifs. Regions of the IOR α subunit show features characteristic of the α , β and δ subunits from POR and VOR (Siddiqui *et al.*, 1997). This information, along with the consideration of the subunit's size, provides evidence that IOR arose through recombination and deletion events. S2 has two homologs to IOR α (MM0451 and MM0123) and two homologs to IOR β (MM0452 and MM0122). MM0123 is larger than

MM0451 by 102 bp, and MM0122 is larger than MM0452 by 30 bp. Additionally, MM0123 appears to contain 2 ferredoxin-like Fe-S cluster motifs (CXXCXXCXXXCP) at the C-terminus, while MM0451 appears to only contain 1 such motif at the C-terminus. There is another possible Fe-S binding motif downstream of the probable Fe-S cluster motif in MM0451, but the proline residue on the end of the motif is replaced by a lysine residue. Because the proline residue is highly conserved in Fe-S cluster motifs, it is not clear that this motif is capable of functioning as an Fe-S binding site.

Strain S2 has one POR. The POR consists of 4 subunits (α , β , δ and γ). These genes are contiguous, and they are arranged in the order γ - δ - α - β (MM1590-MM1589-MM1588-MM1587). This order of arrangement of the POR genes is conserved throughout the methanogens and Archaea. This fact provides a clue that POR is conserved evolutionarily, and this conservation may be evidence that POR is essential.

Strain S2 has one homolog of VOR. MM1348 is the α subunit, and MM1349 is the β subunit. Of particular note is that MM1348 shows greater homology to the β subunits of other oxidoreductases, even though it is the α subunit (i.e., the largest subunit) of VOR. The opposite case is true for MM1349; it shows greater homology to other α subunits than β . Additionally, MM1348 contains a TPP-binding domain. This is significant because TPP-binding domains are found in the β subunits of all oxidoreductase enzyme complexes, with the exception of IOR (i.e., the TPP-binding domain is located in the α subunit)

Another important observation about MM1348 is its size. MM1348 is 1440 bp in length. This is contrasted to the other β subunit homologs in S2 (MM1396, MM0111 and MM1587) which are 795, 867 and 894 bp, respectively. Additionally, the N-terminus of

MM1348 bears homology to the γ subunits in S2 (MM1590 and MM1395), which are 171 residues in length. This indicates that MM1348 is large enough to contain regions that are homologous to both β and γ subunits without any deletions. This is evidence that MM1348 and other large VOR subunits like it may be fusions of the two subunits.

Strain S2 has one homolog of KOR. KOR consists of 3 subunits α , β and γ , and these subunits are represented in strain S2 by MM0642, MM1396 and MM1395, respectively. Interestingly, MM0642 is not contiguous with MM1396 and MM1395. This is opposed to the described KOR genes in *Methanothermobacter thermautotrophicus* strain Δ H, in which the three genes that encode for the three subunits of KOR are contiguous. However, *Methanococcus voltae*, *Methanothermococcus thermolithotrophicus* and *Methanocaldococcus jannaschii* all have the three KOR subunit homologs arrayed in a similar fashion to strain S2: the α subunit homolog is separated from the β and γ subunit homologs.

The functions of MM0112 and MM111 are currently a mystery. These two genes bear only a weak sequence similarity to other OR subunit homologs. However, the two ORFs bear sequence similarity to an OR from *Sulfolobus* that catalyzes the oxidative decarboxylation of a wide range of 2-oxoacid substrates (Fukuda and Wakagi, 2002).

Description of *Methanococcus voltae* OR homologs

As seen in Figure 3.3, *Methanococcus voltae* has two IOR homologs. MV0126 and MV0125 are the IOR α and β subunit homologs, respectively, that best fit what is known about IOR subunits. MV0126 is 599 amino acid residues in length. This is comparable to other IOR α subunit homologs, MTH1852, MM0123 and MM0451, which are 612 amino acid residues, 612 residues and 578 residues in length, respectively.

MV0125, the β subunit homolog, is 188 amino acid residues in length while MTH1853, MM0122 and MM0452 are 196, 199 and 188 amino acids long, respectively.

MV1221 and MV1222 comprise the second IOR α subunit homolog in *M. voltae*. MV1221 and MV1222 appear to be two ORFs. However, MV1221 shows homology to the N-terminal portion of the IOR α subunit in *Methanothermobacter thermautotrophicus* strain Δ H, which is encoded by the gene MTH1852. MV1222 shows homology to the C-terminal portion of the *M. thermautotrophicus* Δ H IOR α subunit. Additionally, MV1222 contains 2 ferredoxin-like Fe-S binding motifs, while MV1221 contains no such motifs. It is possible that MV1221 and MV1222 are in fact a single ORF, and an error in annotation or sequencing may have incorrectly predicted two ORFs. Alternatively, they may be pseudogenes that are not expressed.

M. voltae also possesses POR, VOR and KOR homologs. There are a few remarkable features that are found in these OR homologs that are not found in the ORs of other related organisms. One difference is the KOR α subunit. MV1507 and MV1508 both show homology to other KOR α subunit homologs. The difference is that MV1507 and MV1508 appear to be two genes. This may be due to an error in sequencing or annotation, as MV1507 is homologous to the N-terminal end of other KOR α subunit homologs, and MV1508 is homologous to the C-terminal end.

The *M. voltae* POR homolog ORF cluster, MV0761 through MV0758, is arranged in the same order, γ - δ - α - β , as other POR ORFs from related organisms. However, there is considerable distance (about 100bp) between the end of MV0759 and MV0758, the POR α and β subunit homologs respectively. This suggests that these two

ORFs may not be coexpressed. It is possible that a transcription termination site and a promoter may be present in the 100 bp region between these two ORFs.

MV0284, the VOR α subunit homolog, is separated from the VOR β subunit homolog, MV0285, by approximately 100 bp. MV0286, the γ subunit homolog, is separated from MV0285 by a larger distance (about 150 bp). This suggests (like MV0759 and MV0758) that these ORFs may not be cotranscribed.

Description of *Methanothermococcus thermolithotrophicus* OR homologs

As seen in Figure 3.4. *Methanothermococcus thermolithotrophicus* has 2 POR homologs. This is different from *M. maripaludis*, *M. thermautotrophicus*, *M. voltae* and *M. jannaschii*, which only possess one POR homolog apiece. However, only one of the clusters of ORFs of the POR homologs in *M. thermautotrophicus* have the 2 genes, *por E* and *por F*, commonly associated with the *por* operon in other methanogens.

M. thermolithotrophicus has two KOR homologs. One of the KOR α homologs is not contiguous with a KOR β and a KOR γ homolog, and this is the same case as was seen in the strain S2 as well as the *M. voltae* KOR subunit homologs. However, the other KOR α homolog, MT1569, is contiguous with KOR β and KOR γ homologs (MT1570 and MT1571, respectively). This arrangement of the KOR genes is found in *M. thermautotrophicus*, in which the KOR activity of these genes was previously described.

MT0867 is the MM0112 homolog, and MT0866 is the MM0111 homolog. What is interesting to note is that both MT0867 and MT0866 are upstream of and contiguous with a hydrogenase expression/formation protein gene *hypA* (MT0865). The same case is seen in strain S2, where MM0112 and MM0111 are arranged in a similar orientation with MM0110, another homolog of the *hypA* gene.

A VOR and IOR homolog were not found in the database for *M. thermolithotrophicus*. This could mean that *M. thermolithotrophicus* is unable to synthesize the aromatic and branched-chain amino acids by means of the IOR and VOR reactions, respectively.

Description of *Methanocaldococcus jannaschii* OR homologs

Only 2 OR types are found in *M. jannaschii*. They are POR and KOR, and the maps can be seen in Figure 3.5. The numbers of the ORFs on Figure 3.5 are not the ones assigned by the ERGO database. The numbers are the ORF designations assigned by Bult *et al.* (1996) when the genome was completely sequenced.

There is nothing remarkable about the POR of *M. jannaschii*. The ORFs are arranged in the familiar order of γ - δ - α - β . The KOR, however, has a spatial arrangement of ORFs much like that found in *M. maripaludis* does. The gene encoding the α subunit (MJ0276) is not contiguous with the β (MJ0537) and γ (MJ0536) subunits.

Phylogenetic analysis of 2-oxoacid oxidoreductase α subunit homologs

2-Oxoacid oxidoreductase subunit (OR) α homologs are so named because they are usually the largest of the oxidoreductase subunits. The subunits range in size from ~340 to ~380 amino acids. One exception is MM0112 and MT0867, which are 578 amino acids and 577 amino acids in length, respectively. The results of the phylogenetic analysis of the α homologs are shown in Figure 3.6.

The OR subunit α homologs studied in this work formed 4 different phylogenetic clusters. Four clusters of α subunit homologs were also seen on the Neighbor-joining conserved sequence and nearly complete alignment trees, as well as the Fitch-Margoliash conserved alignment trees (data not shown). Conserved sequence alignment means that

the phylogenetic analysis was performed using only the portion of the alignment that showed the most similarity. Complete sequence alignments are alignments of the entire sequence. Three of the clusters in Figure 3.6 were assigned to POR, VOR and KOR based upon the presence of a *Methanothermobacter* sequence in each cluster. One cluster did not contain a *Methanothermobacter* sequence, and its function is unknown. In other words, all of the subunits in the KOR lineage are thought to have the activity of a KOR α subunit. This reasoning is based on high similarity to biochemically characterized enzymes, and, to a lesser degree, the conservation of functional regions.

The POR lineage, as shown in Figure 3.6, is composed of 6 members. MTH1739 and MM1588 are both known to encode for POR α subunits. MTH1739 is the sole POR α subunit in *Methanothermobacter thermautotrophicus* strain Δ H, and the activity of a homolog was described in *Methanothermobacter marburgensis* (Tersteegen *et al.*, 1997). MM1588 is the sole POR α subunit in *Methanococcus maripaludis*, and its activity was biochemically described as well (Lin, personal communication)

MT1556 is one of 2 POR α homologs in *Methanothermococcus thermolithotrophicus*. Unlike the other POR α homolog, MT0988, MT1556 does not cluster within the POR α homologs from other members of the *Methanococcales* (i.e. *Methanocaldococcus jannaschii*, *Methanococcus voltae* and *Methanococcus maripaludis*). MT1556 is located as a deep branch away from the *Methanococcales* POR α homologs and MTH1739, the POR α homolog in *Methanothermobacter thermautotrophicus*. Of further note is that the contig containing MT1556 lacks the two genes that encode for the two "cysteine-rich" (CR) proteins *porE* and *porF*. All of the other POR α homologs displayed on Figure 3.6 are contiguous with two CR subunits.

One can speculate that the gene cluster that includes MT1556 does not function as an anabolic POR, because the two CR subunits are hypothesized to be responsible for electron transport to the anabolic enzymes. This reasoning is based on the fact that the genes encoding the CR subunits are contiguous with the genes encoding other subunits of the biosynthetic POR enzyme in methanogens and the properties of deletion mutants for these genes (Lin, personal communication).

In methanococci, the genes encoding the KOR α homologs are not contiguous with the genes encoding the β and γ subunits. It is unknown if and how this separation affects the activity of the KOR, but it can be reasoned that KOR is an essential protein because it is needed for the biosynthesis of 2-oxoglutarate, a key intermediate in the pathway to glutamate. Therefore, the separation probably doesn't have an affect on KOR function. However, one cannot rule out the affect the separation of subunits may have on the regulation of transcription.

Among the KOR α homologs shown in Figure 3.6, two belong to *M. thermolithotrophicus*. Like other methanococcal genes that encode KOR α subunit homologs, MT0073 is not found near genes encoding other KOR subunits. However, MT1569 is contiguous with other KOR genes. MT1569 is also more similar to MTH1033 than to any of the other methanococcal genes on the KOR α cluster.

The three members of the VOR β lineage seem to branch from one node, but this is not the case. MTH704 branches from a different node than MM1349 and MV0285. This gene would not be expected to be essential, and it appears to be absent from *M. jannaschii* and *M. thermolithotrophicus*. MT0867 and MM0112 form a separate cluster in this group (Figure 3.6). No function can be assigned to these two ORFs because of

their low similarity to other well described genes. However, there is evidence that these two OR homologs are similar to a *Sulfolobus* OR homolog that catalyzes the oxidative decarboxylation of a wide range of 2-oxoacid substrates (Fukuda and Wakagi, 2002). Enzyme assays performed on purified *Sulfolobus* OR (or SulOFOR) have proven that the enzymes utilizes not only pyruvate, but also 2-oxoglutarate and 2-oxobutyrate also (Zhang *et al.*, 1996).

Phylogenetic analysis of 2-oxoacid oxidoreductase β subunit homologs

The β subunit of 2-oxoacid oxidoreductases contains a TPP-binding motif. The purpose of TPP in the 2-oxoacid oxidoreductase is to bind the substrate, and it does this by forming a carbanion, a negatively charged carbon ion. The β subunit is essential to the enzyme's activity because it contains an important prosthetic group: TPP. The results of the phylogenetic analysis of the β subunits are shown in Figure 3.7.

Like the POR α homologs shown on Figure 3.6, the phylogeny of the POR β subunit homologs formed 4 different branches. The branch with the most members contained MJ0266, MT0989, MM1587 and MV0758. These ORFs were contiguous with the 4 POR α subunit homologs that grouped together.

MT1557 is the gene that encodes a POR β subunit homolog. MT1557 is contiguous with MT1556, the gene that encodes a POR α subunit homolog. Like MT1556, MT1557 occupies a deep branch that is separate from other POR subunit homologs that are found in organisms belonging to *Methanococcales*. In other words, MT1557 is not grouped with MJ0266, MT0989, MM1587 and MV0758. The same speculations that were made about MT1556 can be made with MT1557. MT1557 may be

part of a 2-oxoacid oxidoreductase that is a close relative of the POR but carries out a different function.

The grouping of the subunits in the KOR β cluster is similar to the grouping of the subunits in the KOR α cluster on Figure 3.6. There are 3 lineages in the KOR cluster. One lineage includes the methanococcal ORFs, MT0070, MM1396, MV0725 and MJ0537. The two other lineages have a single member apiece. One includes MTH1034, which is the gene that encodes the KOR β subunit in *Methanothermobacter thermautotrophicus*. The other contains MT1570, which is contiguous with MT1569, the gene that encodes a KOR α subunit homolog in *M. thermolithotrophicus*.

Three subunits which are encoded by the genes MM1348, MV0284 and MTH705 form a separate cluster on Figure 2. The grouping of the three VOR α subunit homologs in Figure 3.7 is similar to the grouping of the three VOR β subunit homologs in Figure 1.

MM0111 and MT0866 are the genes that encode two oxidoreductase β homologs, and MM0111 and MT0866 form a separate cluster in this group (Figure 3.7). No function can be assigned to these two ORFs because of their low similarity to other genes. However, there is evidence that these two OR homologs are similar to a *Sulfolobus* OR homolog that catalyzes the oxidative decarboxylation of a wide range of 2-oxoacid substrates (Fukuda and Wakagi, 2002).

Phylogenetic analysis of 2-oxoacid oxidoreductase γ subunit homologs

Three of the clusters (POR, VOR and KOR) in Figure 3.8 consist of γ subunit homologs that are contiguous with the α and β subunit homologs described in Figures 3.6 and 3.7, respectively. There is no significant change in branching patterns of the members between the POR, VOR and KOR clusters between the three trees. There was

one significant difference in the γ homologs, no "unknown" cluster was found because no oxidoreductase γ homologs were found to be contiguous with either of the unknown oxidoreductase α or β subunit homologs. In addition, an IOR cluster was found.

The IOR cluster on Figure 3.8 contains 3 distinct branches. One of the branches contains a single member, MTH1853. MTH1853 is the gene that encodes for the biochemically described IOR β subunit in *Methanobacterium thermoautotrophicum*. MTH1853 is located on a branch away from the two other branches, which contain methanococcal genes. As stated before, the separation of methanobacterial genes from methanococcal genes on the phylogenetic tree was due the low relatedness of these organisms.

The two other branches in the IOR cluster on Figure 3.8 represent a difference among the IOR homologs. The most notable difference is in the IOR α subunit homologs, which will be discussed below. The IOR β subunit homologs reflect this difference. However, the phylogeny of the IOR β subunits is not supported by as high of bootstrap values as the phylogeny of the IOR α subunit homologs.

Phylogenetic analysis of indolepyruvate oxidoreductase α subunit homologs

IOR α subunits appeared to be fusions of α , β and δ subunits (Siddiqui *et al.*, 1997). However, only weak similarity was found to homologs of the other oxidoreductases, and it was difficult to produce alignments of the IOR subunits with subunits from the other ORs. Therefore, the phylogeny of the IOR α subunits were analyzed separately.

Three phylogenetic clusters of IOR α subunit homologs were found (Figure 3.9). One of these clusters consisted of a single member: MTH1852. MTH1852 is the gene

that encodes for the biochemically characterized IOR α subunit in *Methanothermobacter thermautotrophicus*. Another cluster consisted of MM0123 and MV1221. Both of the subunits encoded by these genes were very similar to MTH1852 in terms of functional domains. Both of the subunits encoded by MM0123 and MV1221 have 2 ferredoxin-like Fe-S cluster binding motifs close to the C-terminus as well as a modified putative thiamine pyrophosphate (TPP) binding motif near the middle of the ORF. Therefore, it is likely that MM0123 and MV1221 encode for an IOR α subunit that is functionally homologous to the IOR α encoded by MTH1852.

The remaining cluster contained IOR α homologs that were encoded by MV0126 and MM0451. These two IOR α homologs are different from the other IOR α homologs. They contain only one putative ferredoxin-like Fe-S cluster binding motif. However, like the IOR α homologs encoded by MM0123, MV1221 and MTH1852, they contain a modified TPP-binding site motif. Therefore, it is unknown if MV0126 and MM0451 encode for an IOR α subunit that is functionally similar to the IOR α subunit encoded by MTH1852.

Phylogenetic analysis of coenzyme F₃₉₀ synthetase homologs

Coenzyme F₄₂₀ functions primarily as an electron carrier in methanogenesis as well as some anabolic reactions (Keltjens *et al.*, 1986). Upon exposure to oxygen, some methanogens were found to convert F₄₂₀ to its 8-hydroxy-AMP and 8-hydroxy-GMP esters, coenzyme F₃₉₀-A and coenzyme F₃₉₀-G, respectively (Gloss and Hausinger, 1988). The sole enzyme that is responsible for the conversion of F₄₂₀ to F₃₉₀ is F₃₉₀ synthase. F₃₉₀ synthase has been hypothesized to be a part of a mechanism methanogenic bacteria use to sense the reduction and oxidation potential of the cell (Vermeij *et al.*, 1995). Of

more importance to this work, coenzyme F₃₉₀ synthase homologs have been found to be contiguous with some of the IOR α homologs.

The F₃₉₀ synthetase homologs were divided into 5 different clusters (Figure 3.10). One of the clusters contained F₃₉₀ synthase homologs encoded by the ORFs MM0453 and MV0748. Both of these ORFs were located immediately upstream of an acetolactate synthase small subunit homolog. However, only MM0453 is contiguous with an ORF that encodes an IOR subunit homolog.

The F₃₉₀ synthetase homologs that are encoded by the putative ORFs MV1188 and MM0813 comprise a second cluster. Both of these ORFs are not located near any ORFs that encode IOR subunit homologs.

MTH1855 and MTH161 comprise a third cluster (Figure 3.10). Only MTH1855 is located near an IOR subunit homolog. MTH1855 is different from MM0453, the ORF that encodes the F₃₉₀ synthetase homolog in *Methanococcus maripaludis*, because MTH1855 is located downstream but on the opposite strand of the IOR genes. MM0453 is located downstream and on the same strand.

MV1224 is the sole member of a fourth cluster in Figure 3.10, and it is located immediately downstream of MV1221-1222 and MV1223, the two parts of an IOR α homolog and an IOR β homolog, respectively. MV1224 is not located near an acetolactate synthase small subunit. This fact may be the reason why MV1224 is not located in the same cluster that MM0453 and MV0748 occupy.

The F₃₉₀ synthetase homolog that is encoded by MTH1528 is located on a distant branch on Figure 3.10. The amino acid sequence derived from MTH1528 bears approximately 95% sequence similarity and an evolutionary distance of approximately

0.08 to the biochemically characterized F₃₉₀ synthase in *Methanothermobacter marburgensis*. Therefore, it is reasonable to assume that MTH1528 encodes an F₃₉₀ synthetase. Since the evolutionary distance between MTH1528 and the other F₃₉₀ synthase homologs is so great, it is likely that the methanococcal homologs are not true F₃₉₀ synthetases and that they catalyze some other activity.

Transformation of *M. maripaludis* strain S2

After evaluation of transformations involving vectors (pIJA03-iorA0451, pIJA03-iorA0123, pIJA03-vorA1348, pIJA03-unk0112, pIJA03-cysS0061 and pIJA03-hdrA1849) designed for single-crossover recombinatory events (data not shown), *M. maripaludis* strain S2 was transformed using pIJA03-iorA0451D and pIJA03-iorA0123D. Figure 3.11 shows how the IOR ORFs were mutagenized using the vectors pIJA03-iorA0451D and pIJA03-iorA0123D. The 2 vectors contain 2 regions that are homologous to sequences in the 123 and 451 IOR ORFs. The inclusion of two regions on each plasmid makes a double crossover event possible.

Table 3.6 lists the efficiencies for the transformations. The vector pIJA03-CR was used as a positive control, and no vector was added as a negative control.

Analysis of the genotype of MM00451 mutants

The genotype of the MM00451 mutant was verified by both PCR screening and Southern hybridization. Figure 3.12 is a gel photograph that shows the results of the PCR screen. Primers for the PCR were complementary to the 3' end of the MM00451 ORF and the 5' end of the *pac* cassette. Lane 3 on the figure is wild-type genomic DNA, and there is no evidence of amplification. Lane 5 is pIJA03-iorA0451D. The plasmid serves as a positive control. Lanes 5-9 show DNA fragments that appear to have the same

molecular weight as the positive control. These apparent mutants are identified in the table below.

Figure 3.13 shows the results of a Southern hybridization of a DIG-labeled probe specific to MM00451 to wild-type and mutant *M. maripaludis* genomic DNA. Lane 1 is a λ /HindIII molecular weight marker. Lane 2 is pIJA03-iorA0451D, and lane 3 is wild-type *M. maripaludis* strain S2 genomic DNA. Lane 4 is 451D #11, an IOR mutant. The anti-DIG antibodies hybridized to DNA bands in the mutants that were approximately 1.0 to 8.0-9.0 kbp larger than the wild-type ones. Such a result is indicative of a *pac* cassette insertion. In lane 2, most of the hybridization takes place at around 3.1-3.2 kbp, like the mutants. However there is also hybridization to 2 lower molecular weight bands. Unspecific digestion seems unlikely because *EcoRV*, the enzyme used to cut the DNA, does not exhibit star activity. One plausible explanation for the 2 bands are that there is some supercoiled, undigested DNA on the membrane. Supercoiled DNA is able to travel faster through gels than relaxed DNA, so this could explain the bands. However, no excess DNA bands were seen on the gel prior to the transfer of DNA to membranes. Regardless, a vast majority of hybridization was seen at the 3.1-3.2 kbp level, and this was the expected result for pIJA03-iorA0451D.

Phenotypic analysis of IOR 451 mutants through growth experiments

Mutants and wild-type *M. maripaludis* strain S2 cells were grown in different media for the purpose of describing a phenotype. Figure 3.14 shows the results of the growth of mutant and wild-type cells on McN, McC and McN + aromatic amino acid derivatives. Five mutants were tested, but only two are included on the graph in order to improve the readability. All of the mutants showed similar growth kinetics to 451D #4

and 451D #8, so 451D #4 and 451D #8 were chosen as a representative of all the mutants.

Both the mutant and wild type cells grew the best on complex medium (McC). The wild-type showed greater growth on McC than the mutant, but the difference between the two growth curves was largely negligible. The mutant and wild-type cells showed similar growth kinetics and cell yields on basal medium (McN). The difference between the wild-type and mutants is seen in the comparison of growth on McN + 5mM p-hydroxyphenylacetate, 5mM indole-3-acetate and 5mM phenylacetate (abbreviated as McN +). The wild-type grew better on McN + than McN, but the wild-type in McN + did not grow as well as on McC. The mutant 451D #4 did not grow on McN + during the experiment. However, 451D #8 grew up after an extended lag phase. In order to check for reversion of 451D #8 back to a wild-type phenotype, a second growth experiment was performed.

Figure 3.15 shows the results of the reversion check. The mutant 451D #8 exhibited growth kinetics similar to the wild-type on McN and McN + media. This is evidence that phenotypic reversion was the cause of the late growth of 451D #8 in the previous experiment (Figure 3.15). If slow growth instead of no growth would have been the actual phenotype, then one would expect to see slow growth in Figure 3.16.

Discussion

The phylogenetic analysis of the *M. maripaludis* strain S2 OR homologs has shown that the organism possesses an ability to interact with a wide range of amino acid derivatives. Since *M. maripaludis* is autotrophic, one could reason that these ORs play a role in amino acid biosynthesis. Of particular interest in this thesis is aromatic amino

acid biosynthesis. Strain S2 possesses two IOR homologs. Since there are differences between the two α subunit homologs (MM00451 and MM00123), it is reasonable to assume that the two ORFs may encode for proteins that have different functions.

Transformations of *M. maripaludis* strain S2 with the plasmid pIJA03-iorA0451D have succeeded in producing mutants of the IOR 451. Genotypic analysis by PCR and Southern hybridization of the mutants has revealed the insertion of the 1.3 kbp *pac* cassette into the chromosome. Phenotypic analysis by growth experiments has revealed a phenotype of no growth in media containing aromatic amino acid derivatives. The cause of this phenotype is a mystery, but there are a few explanations.

One explanation is that the aromatic amino acid derivatives act as signals for the activation of the expression of the IORs in *Methanococcus maripaludis*, and down-regulation of the *de novo* aromatic amino acid biosynthesis pathway. The mutant would be unable to make aromatic amino acids in the presence of the aromatic amino acid derivatives. Presumably, the revertants contained mutations that allowed expression of the *de novo* aromatic amino acid biosynthetic pathway.

A second explanation is that the truncated 451 IOR could act as a disruptive factor in cell metabolic pathways. In other words, the truncated 451 IOR could be damaging cell processes by the nonspecific binding of substrates intended for other enzymes. This may be likely since most of the 451 IOR's TPP-binding domain was removed by mutagenesis, and only 8 residues at the N-terminal end of the domain remain. Of the 8 amino acids not taken out by mutagenesis, 3 (the GDS motif) at the N-terminus are highly conserved in all IOR homologs. The GDS motif may be the "core" of the binding site, and the remaining 40-45 residues may provide a framework.

The above explanations cover some of the most plausible reasons for the observed phenotype. In order to find evidence to support an explanation for a phenotype, extensive enzyme assays must be done. Enzyme assays were attempted on the mutants, but since IOR activity is naturally low in *M. maripaludis*, then it was difficult to arrive at conclusions based on the results that were obtained (data not shown). Future exploration of the mutant IOR 451 may more enzyme assays to interpret the phenotype. Also, work could be done on genes expected to be in the pathway of aromatic amino acid biosynthesis.

Table 3.1: Primer sequences for PCR amplification of OR gene sequences and control sequences for single recombination

ORF #	Forward primer	Reverse primer
MM00451	5'- C(6) <u>AGATCT</u> GCAAAACGAGCAGGATACAAG	5'-(6) <u>TCTAG</u> AGGGAATGCCAGAACGTAGAAT
MM00123	5'-C(6) <u>AGATCT</u> GAACTGCAATTGGGGCCTCAT	5'- C(6) <u>TCTAG</u> AGCACATAAATTGGGGCCT
MM01348	5'- C(6) <u>GGTACC</u> GTCTGTGGCTGTGCGGTAT	5'- C(6) <u>GCTAGC</u> GAACTCCCTGTCCCCAAATC
MM00112	5'- C(6) <u>AGATCT</u> GCAAGAGTTAGGGCGGAAT	5'- C(6) <u>TCTAG</u> AGAGAACTCTAAATCGCCCTG
MM00061	5'- C(6) <u>AGATCT</u> GTACAATACTCACACGATG	5'- C(6) <u>TCTAG</u> ATACAATACTCACACGATG
MM01850	5'- C(6) <u>AGATCT</u> GGGATTGTGAAGCCGTAAAGG	5'- C(6) <u>TCTAG</u> ACATCGTATCCAGTTGCGGTA

Table 3.2: Primer sequences for PCR amplification of IOR gene sequences for double recombination

ORF #	Forward primer	Reverse primer
MM00451	5'- C(6) <u>GGTACCG</u> _AATATCGTCATCGCAGCAGT	5'-C(6) <u>GCTAGCG</u> GAGATGCGTGAACCCTTACAA
MM00123	5'- C(6) <u>GGTACC</u> _GCAGGGTGTCTTTTAGCATC	5'-C(6) <u>GCTAGCG</u> GCTGAAATCCTATCCCTGCT

Table 3.3: Annealing temperatures for primer sets

Primer set	Annealing temperatures
0451FO-0451RE	49°C
0123FO-0123RE	55°C
1348FO-1384RE	55°C
0112FO-0112RE	52°C
0061FO-0061RE	48°C
1850FO-1850RE	52°C

Table 3.4: Vector information

Vector	Size (in base pairs)	Function
pIJA03	3470	Original vector
pIJA03-iorA0451	4384	Single insertion mutagenesis of the IOR 0451
pIJA03-iorA0123	4391	Single insertion mutagenesis of the IOR 0123
pIJA03-vorA1348	4220	Single insertion mutagenesis of the VOR 1348
pIJA03-unk0112	4378	Single insertion mutagenesis of the OR 0112
pIJA03-cysS0061	4386	Single insertion mutagenesis of the <i>cysS</i> 0061
pIJA03-hdrA1850	4406	Single insertion mutagenesis of the <i>hdrA</i> 1850
pIJA03-iorA0451D	5218	Double insertion mutagenesis of the IOR 0451
pIJA03-iorA0123D	5358	Double insertion mutagenesis of the IOR 0123

Table 3.5: Primers used for verification of mutant genotype

Primer name	Sequence	Function
check-Pur1	5'-CGCACCGTGGGCTTGTACTC	hybridizes to a 5' region of <i>pac</i>
0451SF	5'-GTTGCAGTTATCGGGGATTCTACGTTCTGG	hybridizes to a 3' region of MM00451
0123SF	5'-ATAATTCCAATTCCCGTAAGGCCCCCAAAT	hybridizes to a 3'-region of MM00123

Table 3.6: Transformation efficiencies in *M. maripaludis* strain S2

vector	Transformation efficiency (transformants/culture)
pIJA03-iorA0451D	862.5
pIJA03-iorA0123D	187.5
pIJA03-CR	362.5
no vector	0

Table 3.7: Identities of *iorA* 0451 mutants in *M. maripaludis* strain S2

Lane (in Figure 3.12)	Identity
3	451D #2
4	451D #4
5	451D #8
6	451D #9
7	451D #11

Figure 3.1: Putative 2-oxoacid oxidoreductase genes in *Methanothermobacter thermautotrophicus* strain Δ H

Genes are shaded according to homology. Black = iorA-alpha subunit; blue = oxidoreductase alpha subunit; yellow = oxidoreductase beta subunit; brown = oxidoreductase gamma subunit; green = oxidoreductase delta subunit. The ORF numbers are the designations assigned by Smith, et al. (1997). The sequences of the genes were found on the ERGO database maintained by Integrated Genomics.

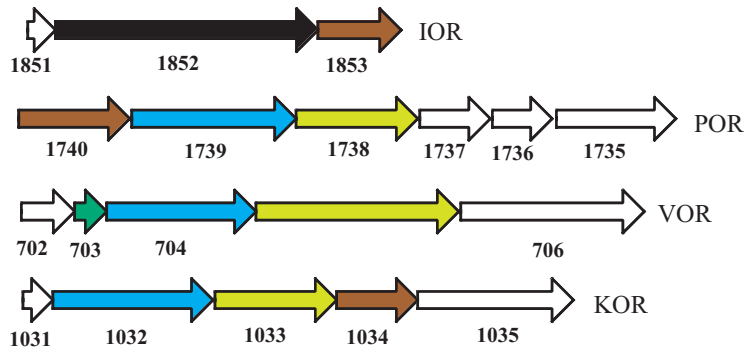


Table 3.8: ORF annotation and homology in *Methanothermobacter thermautotrophicus* strain ΔH

ORF number	Annotation	Homolog
1851	hypothetical protein	
1852	IOR α	IOR α
1853	IOR β	IOR β
1740	POR γ	POR γ and POR δ
1739	POR α	POR α
1738	POR β	POR β
1737	formate hydrogenlyase subunit 2	
1736	formate dehydrogenase alpha chain	
1735	L (+)-tartrate dehydrogenase	
702	acetyl-CoA synthetase	
703	oxygen-insensitive NAD(P)H nitroreductase	VOR γ
704	pyruvate synthase alpha chain	VOR β
705	VOR α	VOR α
706	L-aspartyl-tRNA(Asn)-dependent amidotransferase subunit A	
1031	ferredoxin	
1032	POR α	KOR α
1033	POR β	KOR β
1034	POR γ	KOR γ
1035	succinyl-CoA synthetase beta chain	

The table above lists the annotations and homologies of the ORFs described in Figure 3.1. The annotations for the ORFs are the ones given on the ERGO database (Integrated Genomics). The homologies are used to signify what group of oxidoreductase types and subunits the ORFs fit best in. Contigs are separated by dark lines.

Figure 3.2: Putative 2-oxoacid oxidoreductase ORFs in *Methanococcus maripaludis* strain S2

Genes are shaded according to homology. Black = iorA-alpha subunit; blue = oxidoreductase alpha subunit; yellow = oxidoreductase beta subunit; brown = oxidoreductase gamma subunit; green = oxidoreductase delta subunit. All ORF designation numbers are from the ERGO database. The arrows with lines inside are coenzyme F₃₉₀ synthetase homologs. All numbers are the ORF designations on the ERGO database (Integrated Genomics).

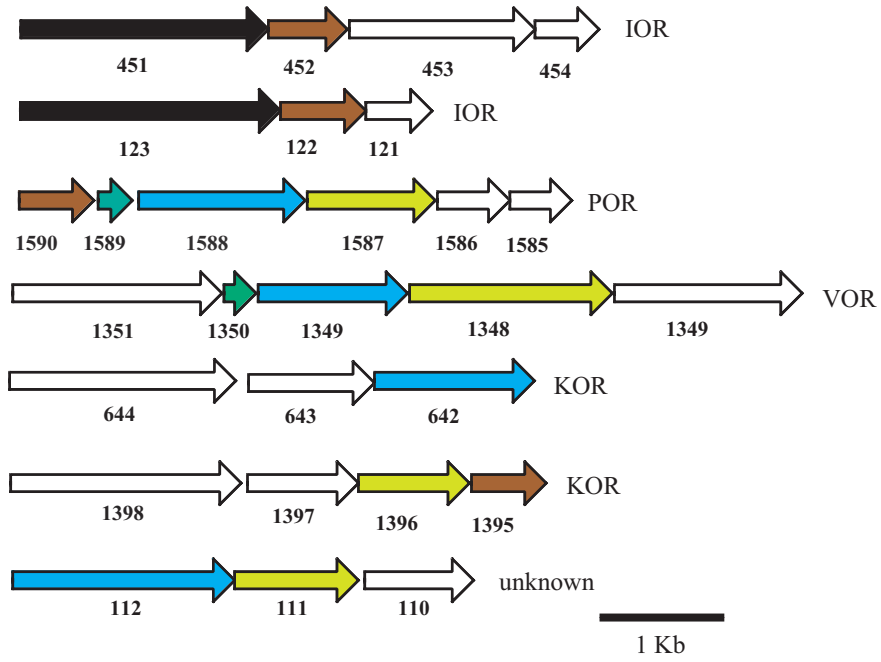


Table 3.9: ORF annotation and homology in *Methanococcus maripaludis* strain S2

ORF number	Annotation	Homolog
451	IOR α	IOR α
452	IOR β	IOR β
453	coenzyme F ₃₉₀ synthetase	
454	acetolactate synthase small subunit	
123	IOR α	IOR α
122	IOR β	IOR β
121	unknown	
1590	POR γ	POR γ
1589	POR δ	POR δ
1588	POR α	POR α
1587	POR β	POR β
1586	formate hydrogenlyase subunit 2	
1585	formate dehydrogenase alpha chain	
1351	acetyl-CoA synthetase	
1350	oxygen-insensitive NAD(P)H nitroreductase	VOR γ
1349	pyruvate synthase alpha chain	VOR β
1348	VOR α	VOR α
1347	hexulose-6-phosphate synthase	
644	unknown	
643	serine/threonine protein kinases	
642	KOR α	KOR α
1398	class 1 lysyl-tRNA synthetase	
1397	nucleotidyl transferase	
1396	POR β	KOR β
1395	POR γ	KOR γ
112	pyruvate synthase alpha chain	unknown OR type (α subunit)
111	POR β	unknown OR type (β subunit)
110	hydrogenase expression/formation protein (<i>hypA</i>)	

The table above lists the annotations and homologies of the ORFs described in Figure 3.2. The annotations for the ORFs are the ones given on the ERGO database (Integrated Genomics). The homologies are used to signify what group of oxidoreductase types and subunits the ORFs fit best in. Contigs are separated by dark lines.

Figure 3.3: Putative 2-oxoacid oxidoreductases in *Methanococcus voltae*

Genes are shaded according to homology. Black = iorA-alpha subunit; blue = oxidoreductase alpha subunit; yellow = oxidoreductase beta subunit; brown = oxidoreductase gamma subunit; green = oxidoreductase delta subunit. The arrows with lines inside are coenzyme F₃₉₀ synthetase homologs. All numbers are the ORF designations on the ERGO database (Integrated Genomics).

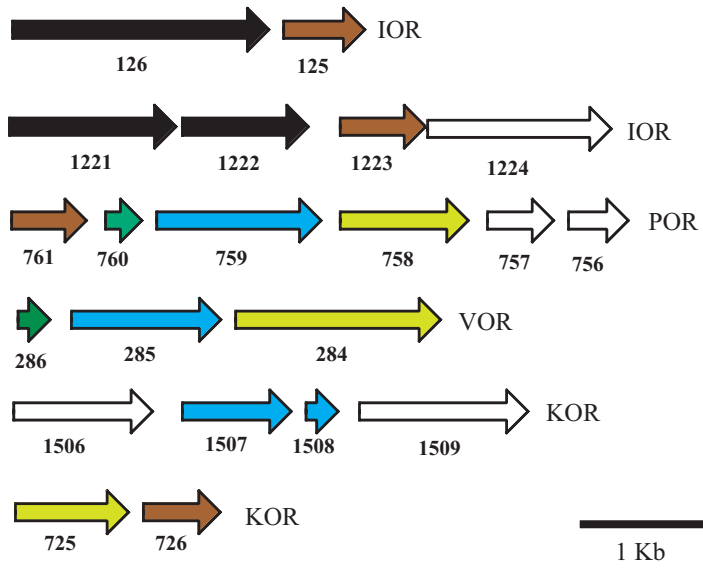


Table 3.10: ORF annotation and homology in *Methanococcus voltae*

ORF number	Annotation	Homolog
126	IOR α	IOR α
125	IOR β	IOR β
1221	IOR α	IOR α
1222	IOR α	IOR α
1223	IOR β	IOR β
1224	coenzyme F ₃₉₀ synthetase	
761	POR γ	POR γ
760	POR δ	POR δ
759	POR α	POR α
758	POR β	POR β
757	formate hydrogenlyase subunit 2	
756	formate dehydrogenase alpha chain	
286	VOR γ	VOR γ
285	VOR β	VOR β
284	VOR α	VOR α
1506	potassium channel protein	
1507	KOR α	KOR α
1508	KOR α	KOR α
1509	L-seryl-tRNA selenium transferase	
725	POR β	KOR β
726	POR γ	KOR γ

The table above lists the annotations and homologies of the ORFs described in Figure 3.3. The annotations for the ORFs are the ones given on the ERGO database (Integrated Genomics). The homologies are used to signify what group of oxidoreductase types and subunits the ORFs fit best in. Contigs are separated by dark lines.

Figure 3.4: Putative 2-oxoacid oxidoreductases in *Methanothermococcus thermolithotrophicus*

Genes are shaded according to homology. Blue = oxidoreductase alpha subunit; yellow = oxidoreductase beta subunit; brown = oxidoreductase gamma subunit; green = oxidoreductase delta subunit. All numbers are the ORF designations on the ERGO database (Integrated Genomics).

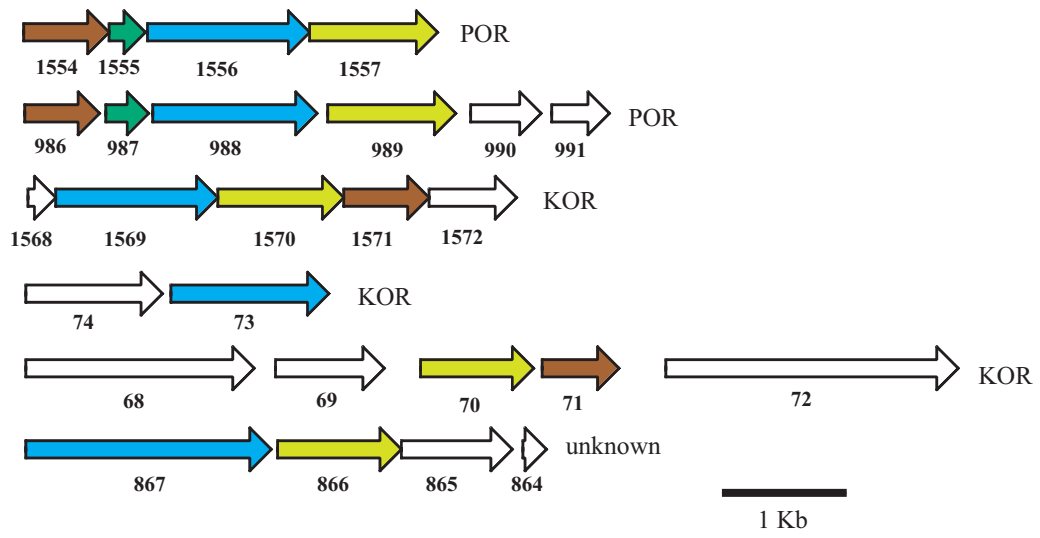


Table 3.11: ORF annotation and homology in *Methanothermococcus thermolithotrophicus*

ORF number	Annotation	Homolog
1554	POR γ	POR γ
1555	POR δ	POR δ
1556	POR α	POR α
1557	POR β	POR β
986	POR γ	POR γ
987	POR δ	POR δ
988	POR α	POR α
989	POR β	POR β
990	formate hydrogenlyase subunit 2	
991	formate dehydrogenase alpha chain	
1568	ferredoxin	
1569	POR α	KOR α
1570	POR β	KOR β
1571	POR γ	KOR γ
1572	carbonic anhydrase	
74	serine/threonine protein kinases	
73	KOR α	KOR α
68	class 1 lysyl-tRNA synthetase	
69	nucleotidyl transferase	
70	POR β	KOR β
71	POR γ	KOR γ
72	archaeal zinc-finger domain protein	
867	pyruvate synthase alpha chain	unknown OR type (α subunit)
866	POR β	unknown OR type (β subunit)
865	hydrogenase expression/formation protein (<i>hypA</i>)	
864	rubredoxin	

The table above lists the annotations and homologies of the ORFs described in Figure 3.4. The annotations for the ORFs are the ones given on the ERGO database (Integrated Genomics). The homologies are used to signify what group of oxidoreductase types and subunits the ORFs fit best in. Contigs are separated by dark lines.

Figure 3.5: Putative 2-oxoacid oxidoreductase genes in *Methanocaldococcus jannaschii*

Genes are shaded according to homology. Blue = oxidoreductase alpha subunit; yellow = oxidoreductase beta subunit; brown = oxidoreductase gamma subunit; green = oxidoreductase delta subunit. All numbers are the ORF designations provided by Bult *et al.* (1996) and not the ERGO database numbers (Integrated Genomics).

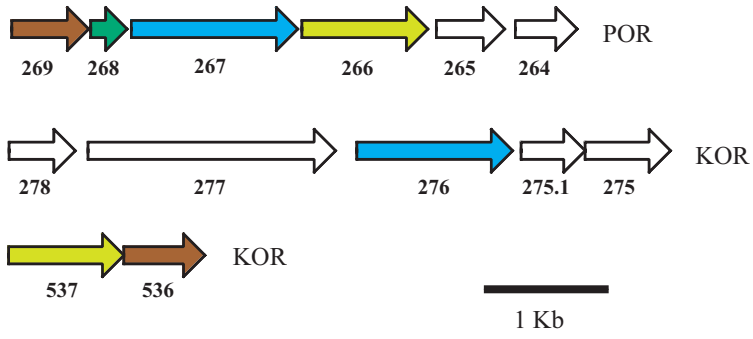


Table 3.12: ORF annotation and homology in *Methanocaldococcus jannaschii*

ORF number	Annotation	Homolog
269	POR γ	POR γ
268	POR δ	POR δ
267	POR α	POR α
266	POR β	POR β
265	formate hydrogenlyase subunit 2	
264	formate dehydrogenase alpha chain	
278	peptidyl-prolyl cis-trans isomerase	
277	acetolactate synthase large subunit	
276	pyruvate synthase alpha chain	KOR α
275.1	hypothetical protein	
275	hypothetical exported protein	
537	POR β	KOR β
536	POR γ	KOR γ

The table above lists the annotations and homologies of the ORFs described in Figure 3.5. The annotations for the ORFs are the ones given on the ERGO database (Integrated Genomics). The homologies are used to signify what group of oxidoreductase types and subunits the ORFs fit best in. Contigs are separated by dark lines.

Figure 3.6: Phylogenetic analysis of oxidoreductase alpha subunit homologs.

The tree shown is based on 284 positions and calculated by the Fitch:Margoliash algorithm of PHYLIP 3.572. Closed circles represent bootstrapping values of >80%, and open circles represent bootstrapping values >60%. POR is the pyruvate oxidoreductase, VOR is the 2-oxoisovalerate oxidoreductase, KOR is the 2-oxoglutarate oxidoreductase. mm is *Methanococcus maripaludis*, mv is *Methanococcus voltae*, mt is *Methanothermococcus thermolithotrophicus*, mj is *Methanocaldococcus jannaschii* and mth is *Methanothermobacter thermautotrophicum*. The beta subunit of VOR is homologous to the alpha subunits of the other oxidoreductases. Similar results were obtained with a Neighbor-joining analysis of the same alignment and Fitch-Margoliash and Neighbor-joining analysis of a conserved sequence alignment.

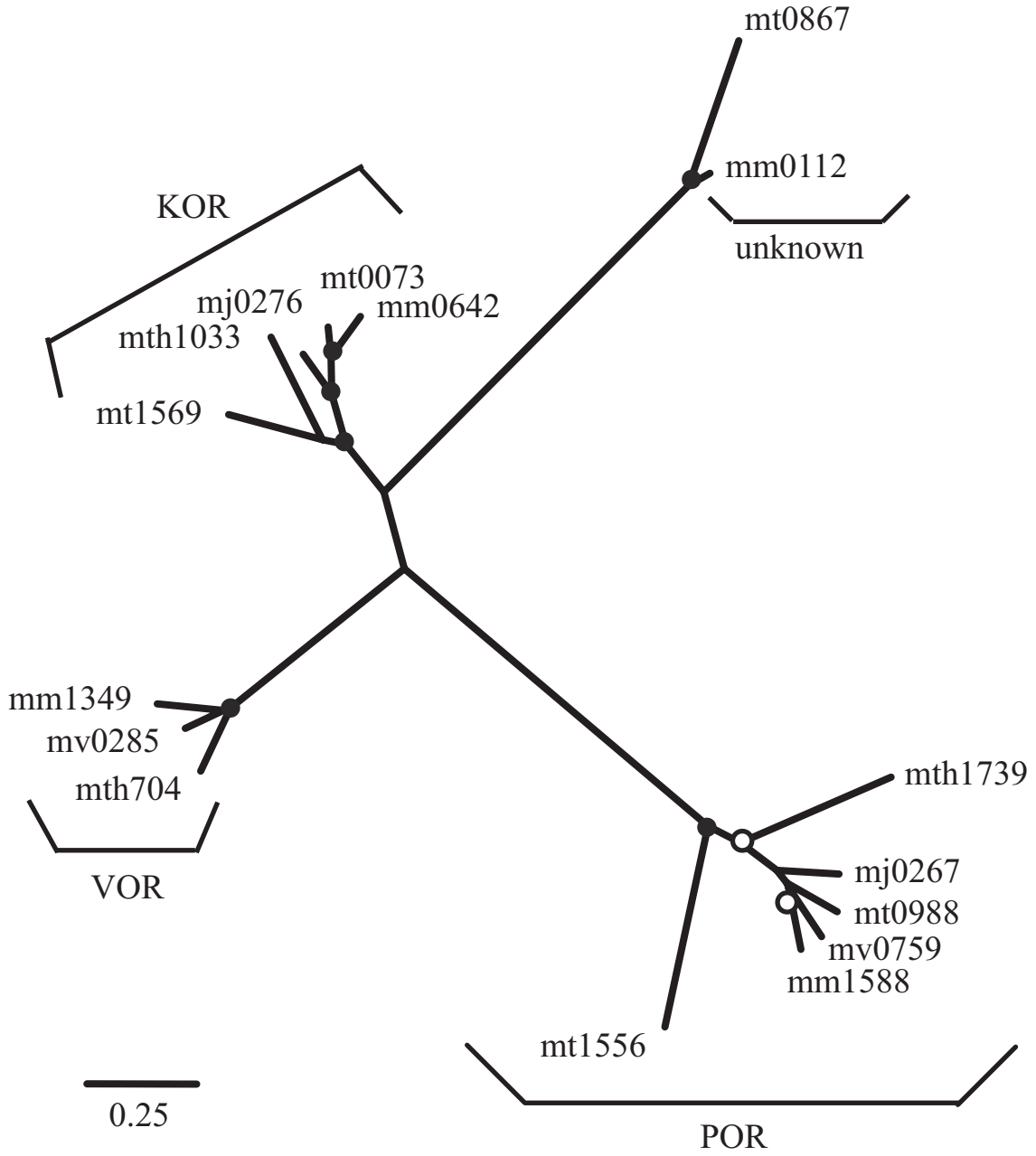


Figure 3.7: Phylogenetic analysis of oxidoreductase beta subunit homologs.

The tree shown is based on 240 positions and calculated by the Fitch:Margoliash algorithm of PHYLIP 3.572. Closed circles represent bootstrapping values of >80%. POR is the pyruvate oxidoreductase, VOR is the 2-oxoisovalerate oxidoreductase, KOR is the 2-oxoglutarate oxidoreductase. mm is *Methanococcus maripaludis*, mv is *Methanococcus voltae*, mt is *Methanothermococcus thermolithotrophicus*, mj is *Methanocaldococcus jannaschii* and mth is *Methanothermobacter thermautotrophicum*. The alpha subunit of VOR is homologous to the beta subunits of the other oxidoreductases. Similar results were obtained with a Neighbor-joining analysis of the same alignment and Fitch-Margoliash and Neighbor-joining analysis of a conserved sequence alignment.

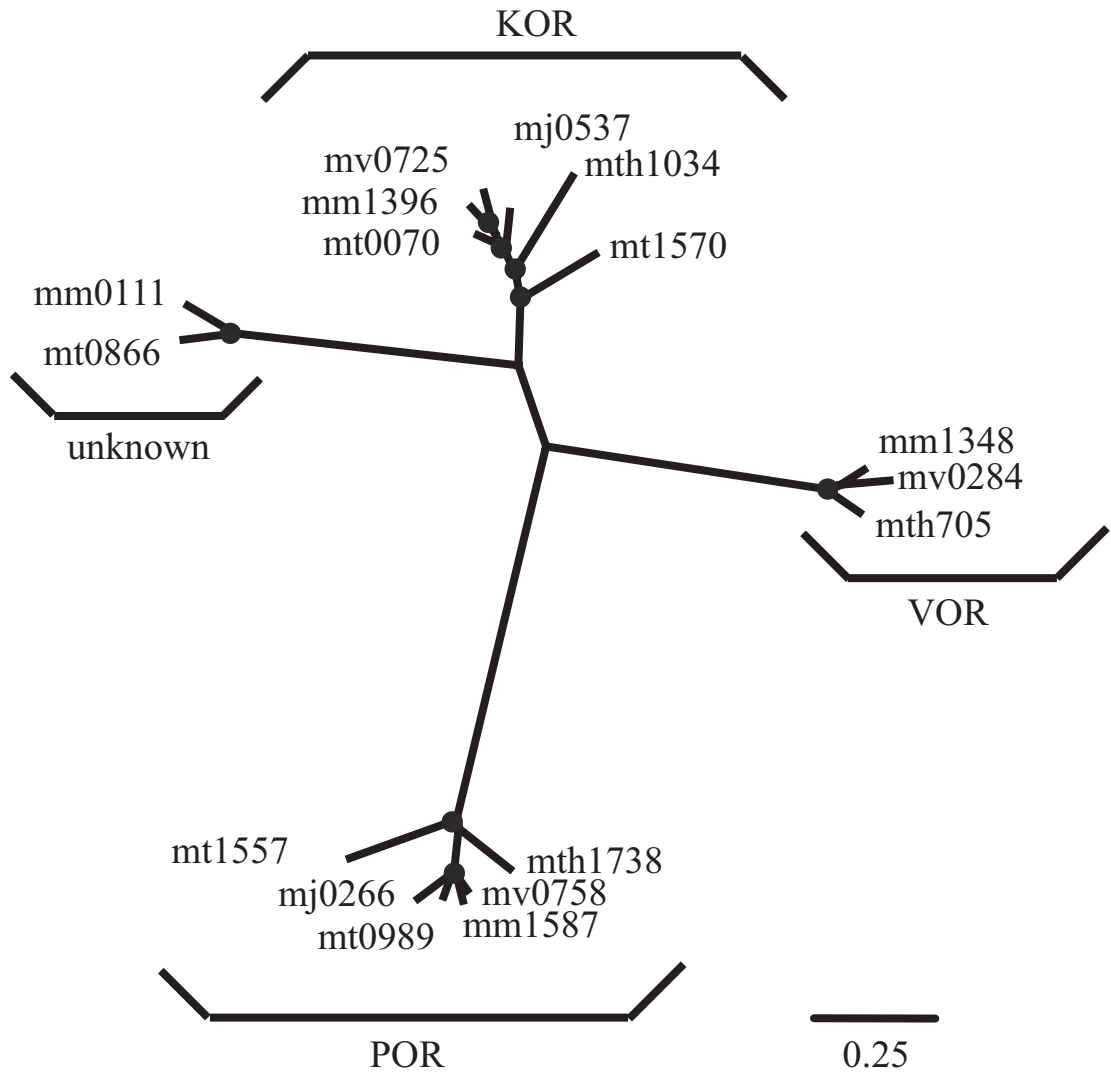


Figure 3.8: Phylogenetic analysis of oxidoreductase gamma subunit homologs.

The tree shown is based on 100 positions and calculated by the Fitch:Margoliash algorithm of PHYLIP 3.572. Closed circles represent bootstrapping values of >80%, and open circles represent bootstrapping values >60%. POR is the pyruvate oxidoreductase, VOR is the 2-oxoisovalerate oxidoreductase, KOR is the 2-oxoglutarate oxidoreductase. mm is *Methanococcus maripaludis*, mv is *Methanococcus voltae*, mt is *Methanothermococcus thermolithotrophicus*, mj is *Methanocaldococcus jannaschii* and mth is *Methanothermobacter thermautotrophicus*. The IOR beta subunits included on the figure are homologous to the gamma subunits of the other oxidoreductases. Similar results were obtained with a Neighbor-joining analysis of the same alignment and Fitch-Margoliash and Neighbor-joining analysis of a conserved sequence alignment.

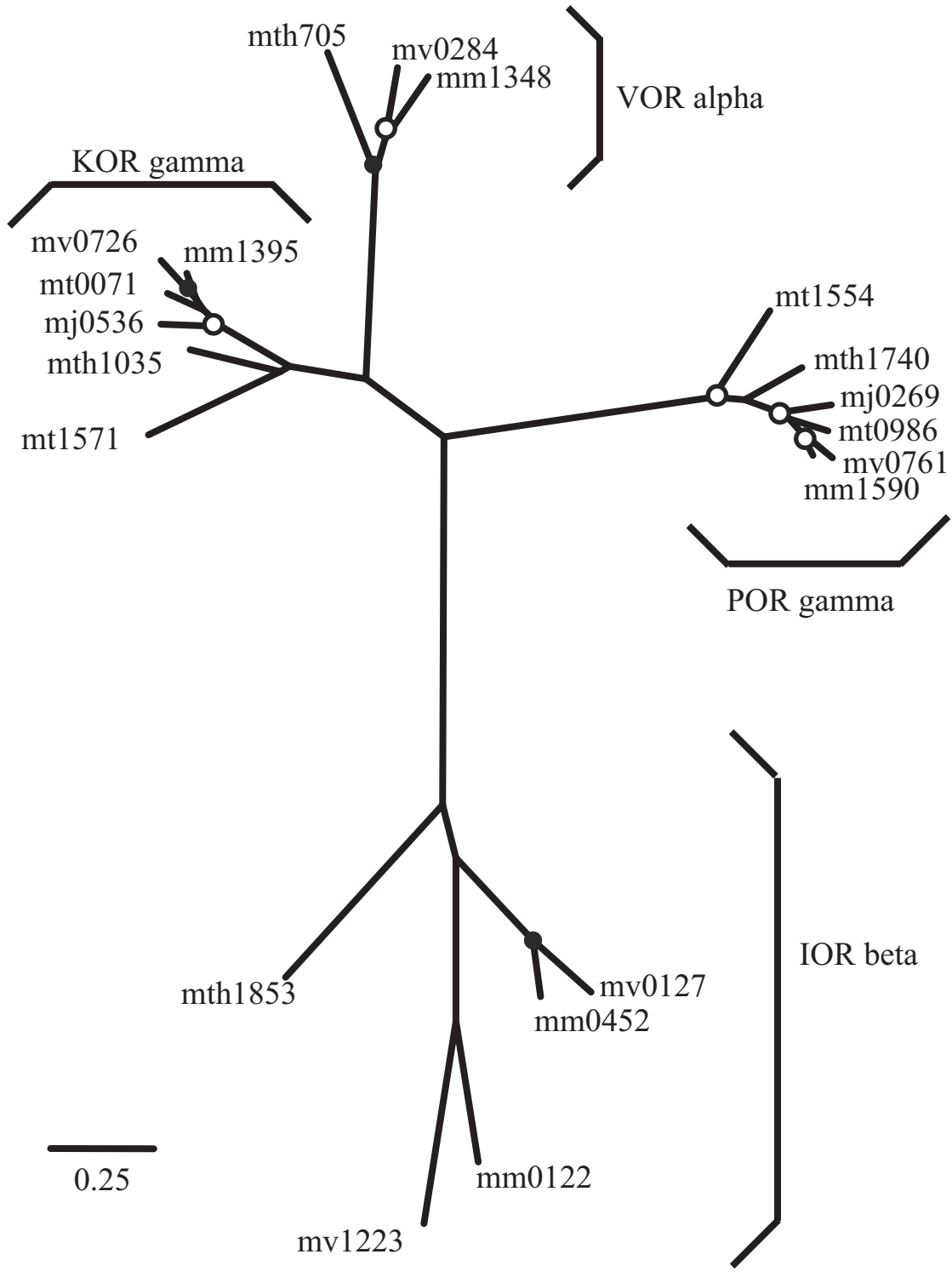


Figure 3.9: Phylogenetic analysis of indolepyruvate oxidoreductase alpha subunit homologs.

The tree shown is based on 581 positions and calculated by the Fitch:Margoliash algorithm of PHYLIP 3.572. Closed circles represent bootstrapping values of >80%. mm is *Methanococcus maripaludis*, mv is *Methanococcus voltae* and mth is *Methanothermobacter thermautotrophicum*. Similar results were obtained with a Neighbor-joining analysis of the same alignment and Fitch-Margoliash and Neighbor-joining analysis of a conserved sequence alignment.

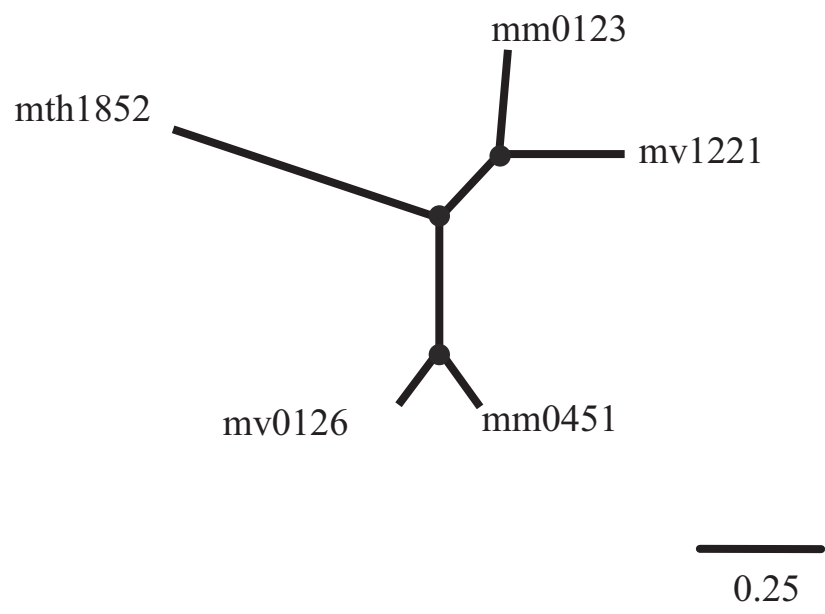


Figure 3.10: Phylogenetic analysis of coenzyme F₃₉₀ synthetase homologs.

The tree shown is based on 150+ positions and calculated by the Fitch:Margoliash algorithm of PHYLIP 3.572. Closed circles represent bootstrapping values of >80%, and open circles represent bootstrapping values >60%. Similar results were obtained with a Neighbor-joining analysis of the same alignment and Fitch-Margoliash and Neighbor-joining analysis of a conserved sequence alignment.

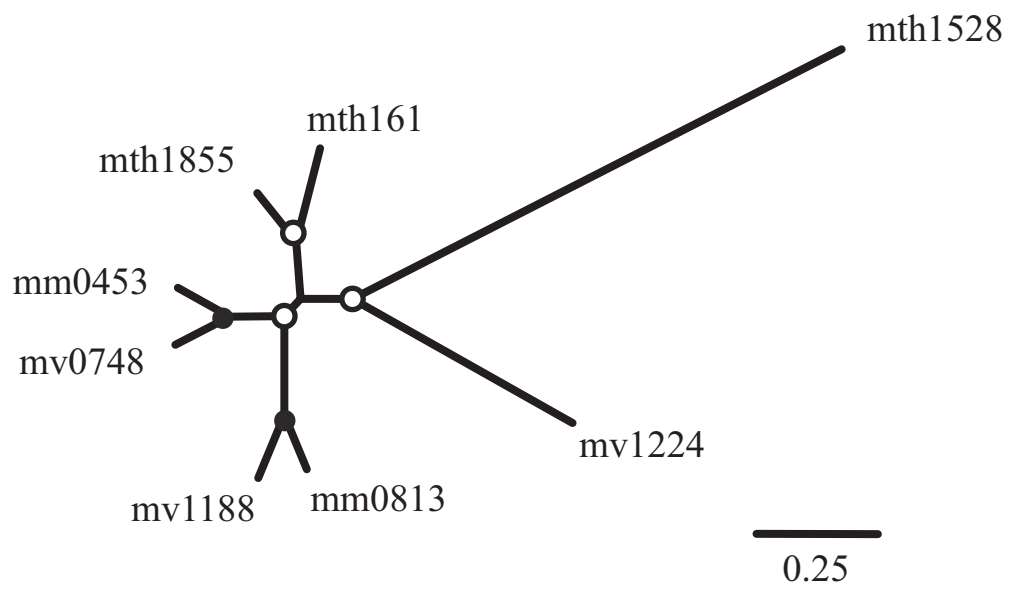


Figure 3.11: Insertional mutagenesis of MM00451 by pIJA03-iorA0451D

Insertional mutagenesis of MM00451 was accomplished by a double crossover event using the “451 up” segment of pIJA03-iorA0451D and the “451 down” segment that bears homology to all of MM00452 and the first 200 bp of MM00453. The pac (1.3 kbp) cassette takes the place of approximately 500 bp at the 3’ end of MM00451.

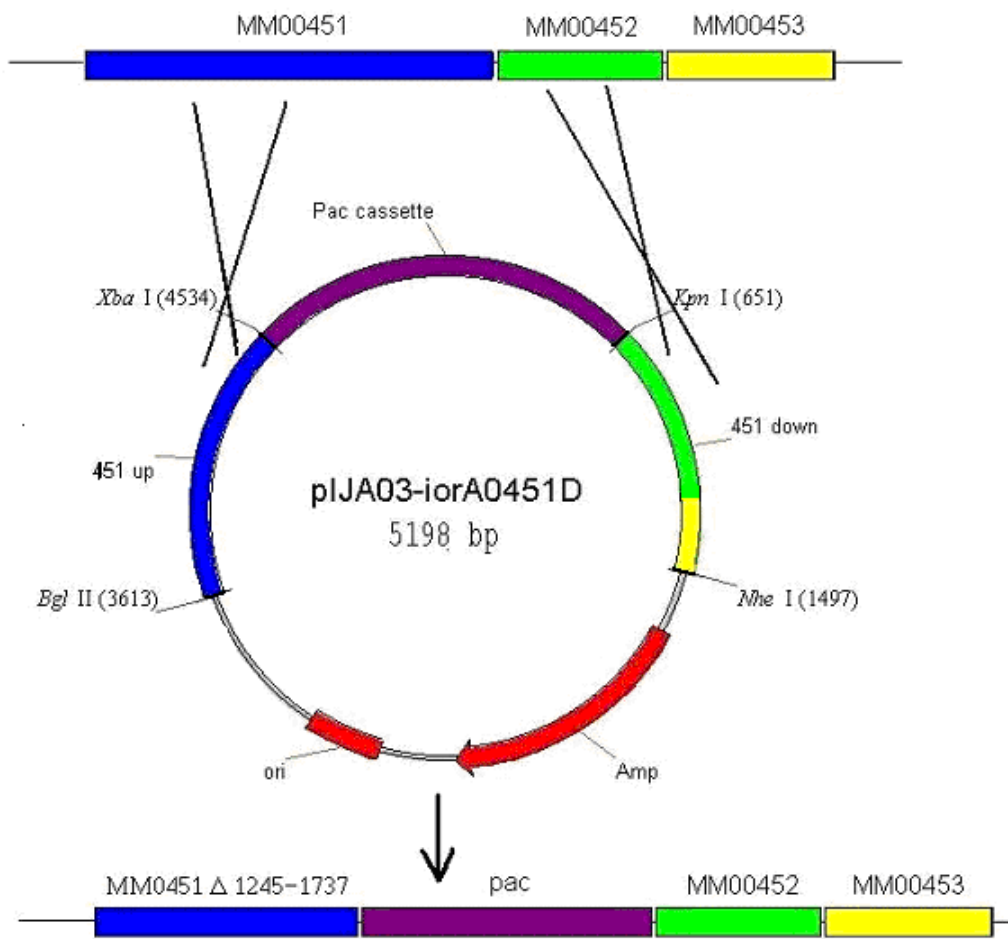


Figure 3.12: Gel electrophoresis of wild-type and 451 IOR mutant genomic DNA PCR products

The figure above shows the electrophoresis of PCR products on a 1 % agarose gel. Primers were made to hybridize to the 3' region of MM00451 (0451SF) and the 5' region of the pac cassette (check-Pur1). Lane 1 is a λ /*Hind* III molecular weight marker. Lane 2 is wild-type genomic DNA. Lane 3 is pIJA03-iorA0451D. Lanes 4-8 are 451D #2, 451D #4, 451D #8, 451D #9 and 451D #11 in that order. The faint bands below the bright bands of PCR product are unextended primer.

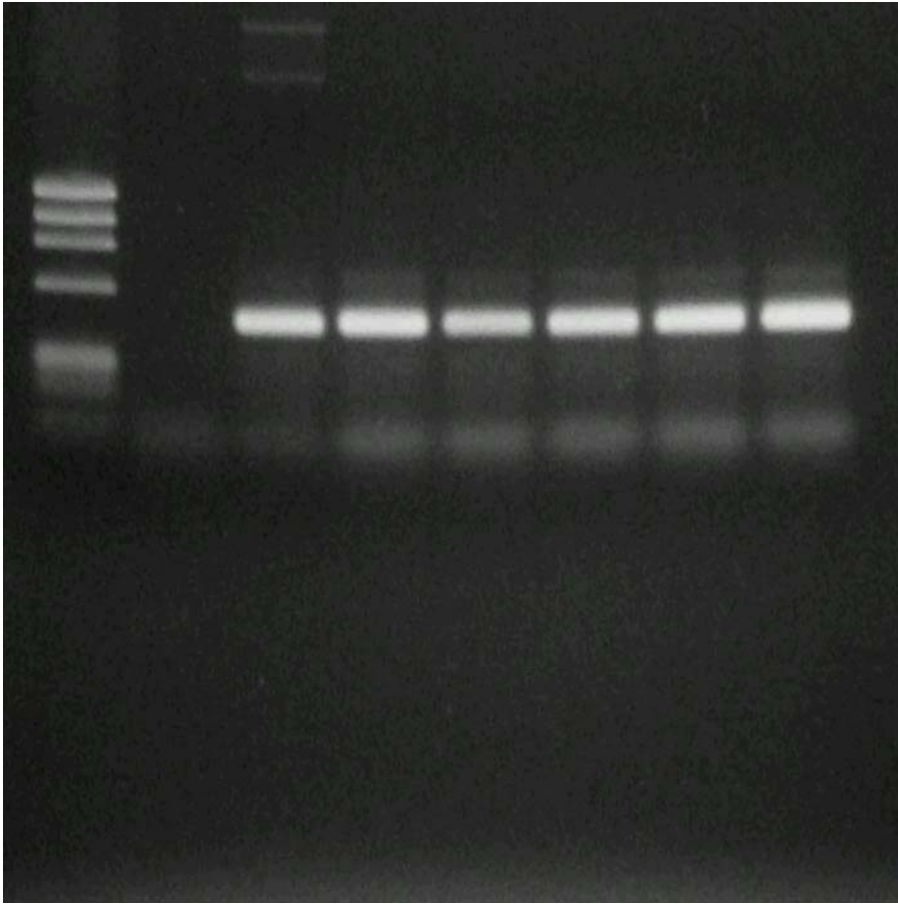


Figure 3.13: Southern hybridization analysis of wild type and 451 IOR mutant *Methanococcus maripaludis* strain S2 genomic DNA

The Southern blot pictured above was done using anti-DIG antibodies. Lane 1 is a λ *Hind*III molecular standard. Lane 2 is pIJA03-iorA0451D. Lane 3 is wild-type strain S2 genomic DNA. Lanes 4-8 are the mutants 451D #2, 451D #4, 451D #8, 451D #9 and 451D #11 in order. The DIG-labeled probes were hybridized to 900 bp of the ORF MM00451 overnight at 65° C. A chromophore was bound to the anti-DIG antibody, and the black areas on the figure above are indicative of bound chromophore.

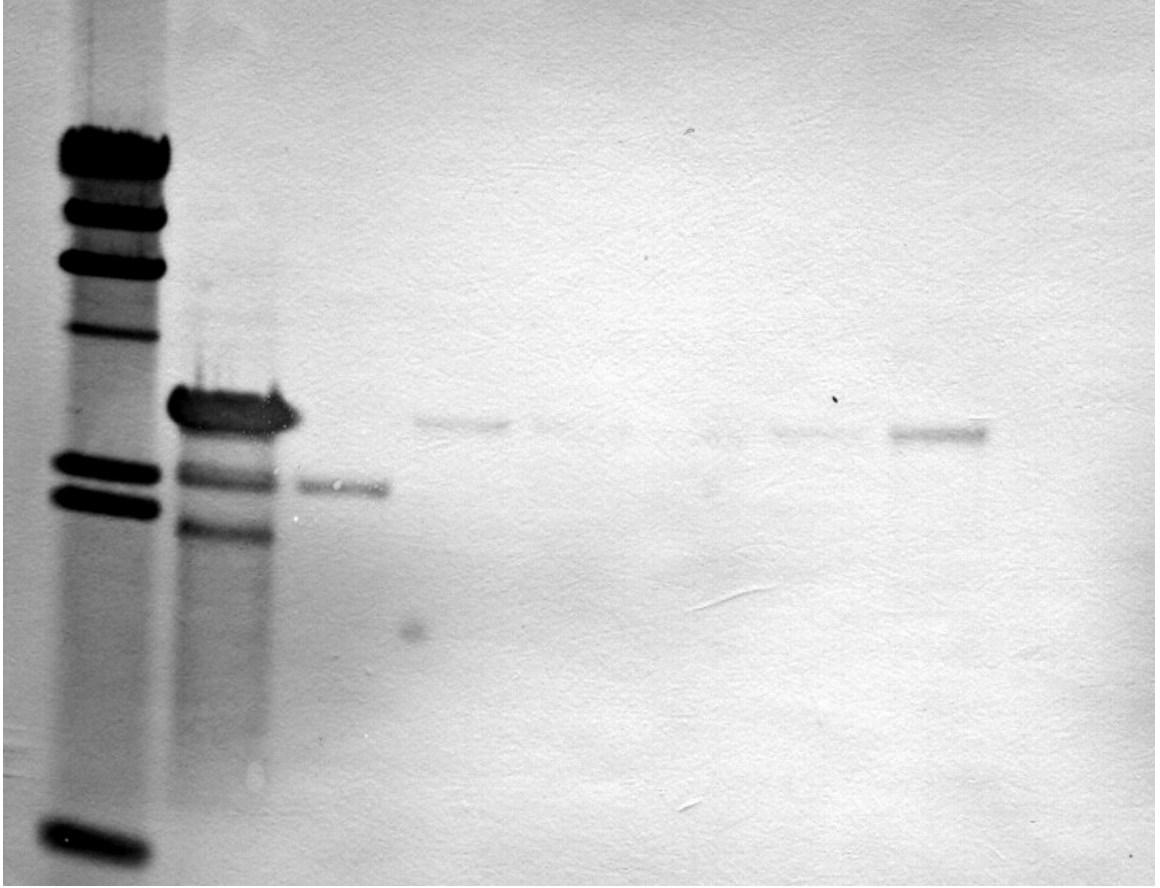


Figure 3.14: Growth of wild-type and mutant *Methanococcus maripaludis* strain S2 on McN, McN + aromatic amino acid derivatives and McC

The above graph shows the growth of wild-type and mutant strain S2 in minimal medium (McN), minimal medium + 5mM p-hydroxyphenylacetate, 5mM indole-3-acetate and 5mM phenylacetate (McN +) and complex medium (McC). All culture tubes were regularly repressurized. The mutant 451D #8 was included on the graph to illustrate the delayed growth that some of the mutants showed.

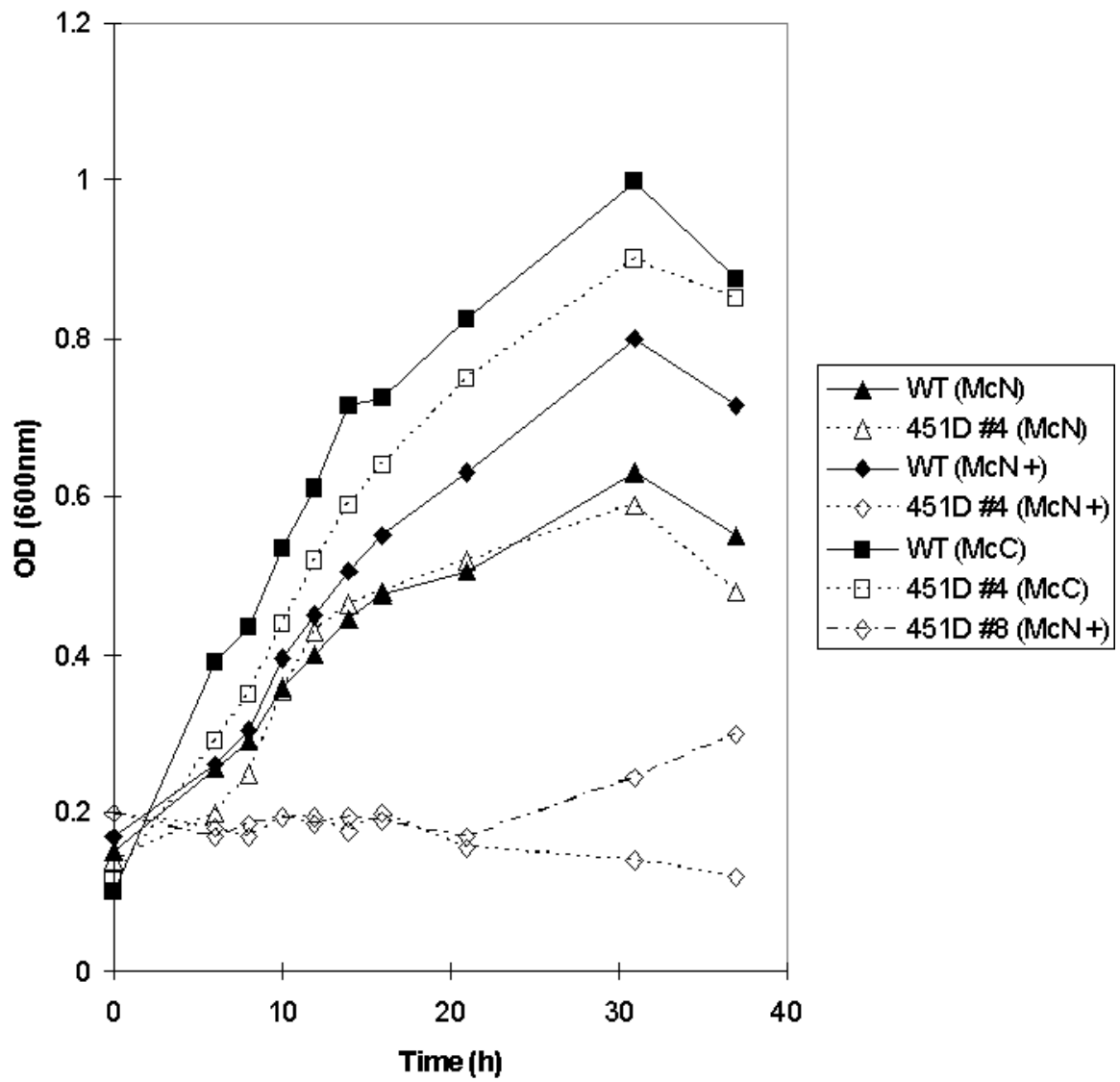


Figure 3.15: Reversion growth experiment of wild-type and 451D #8 mutant *Methanococcus maripaludis* strain S2 in McN and McN + aromatic amino acid derivatives

The above graph shows the growth of wild-type and the mutant 451D #8 in minimal medium (McN) and minimal medium + 5mM p-hydroxyphenylacetate, 5mM indole-3-acetate, 5mM phenylacetate (McN +). All culture tubes were regularly repressurized. This experiment was done to check for a reversion to the wild-type phenotype in a mutant that showed delayed growth.

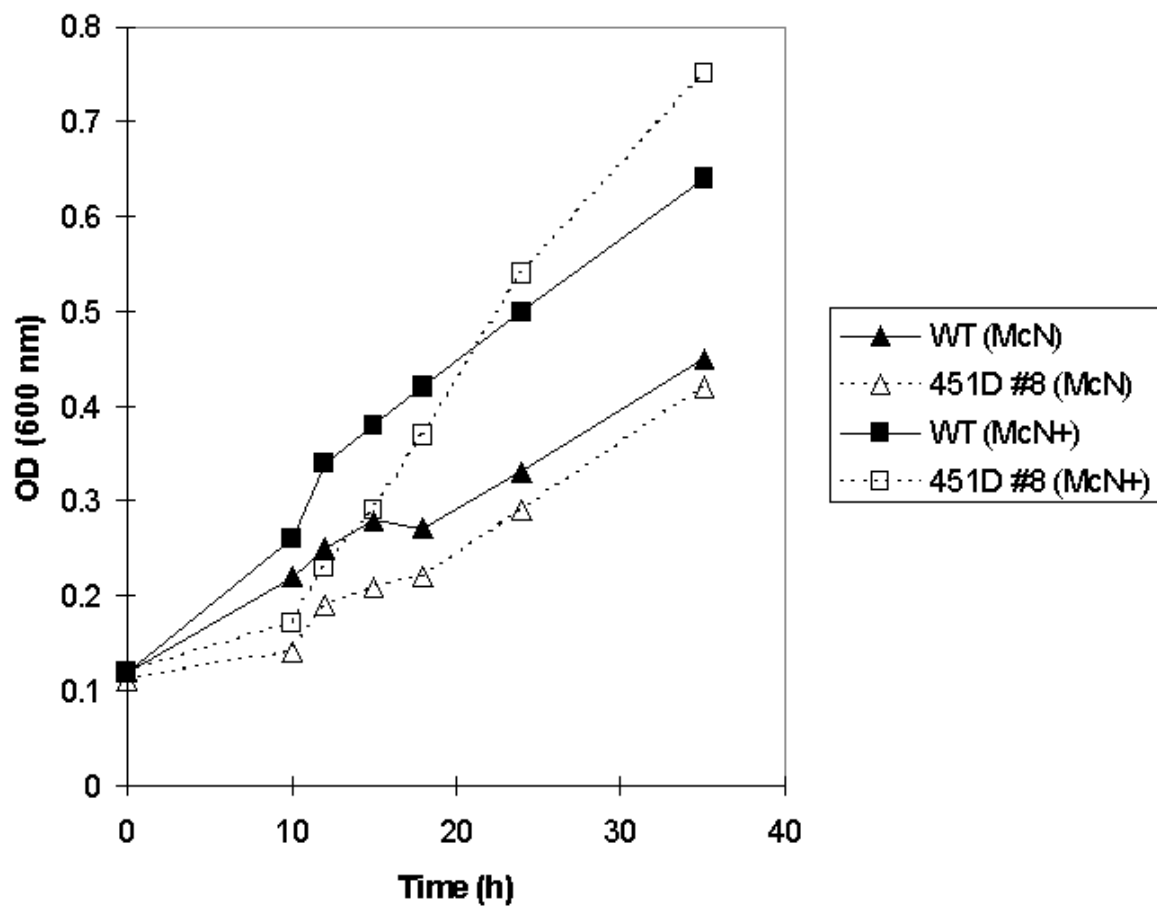


Table 3.13: Commonly used abbreviations

Abbreviation	Full name
TPP	thiamin pyrophosphate
POR	pyruvate oxidoreductase
KOR	2-oxoglutarate oxidoreductase
VOR	2-oxoisovalerate oxidoreductase
IOR	indolepyruvate oxidoreductase
BCAA	branched-chain amino acids
AHAS	acetohydroxy acid synthase
FAD	flavin adenine dinucleotide
H ₄ MPT	tetrahydromethanopterin
MFR	methanofuran
FDH	formate dehydrogenase
CoM	coenzyme M

REFERENCES

- Altschul, S. F., W. Gish, W. Miller, E. W. Myers and D. J. Lipman (1990). Basic local alignment search tool. *J Mol Biol* **215**(3): 403-10.
- Ankel-Fuchs, D. and R. K. Thauer (1986). Methane formation from methyl-coenzyme M in a system containing methyl-coenzyme M reductase, component B and reduced cobalamin. *Eur J Biochem* **156**(1): 171-7.
- Balch, W. E., G. E. Fox, L. J. Magrum, C. R. Woese and R. S. Wolfe (1979). Methanogens: reevaluation of a unique biological group. *Microbiol Rev* **43**(2): 260-96.
- Bock, A. K. and O. Kandler (1985). Antibiotic sensitivity of archaeobacteria. The Bacteria. C. R. Woese and R. S. Wolfe. New York, Academic Press. **8**: 525-544.
- Bock, A. K., P. Schönheit and M. Teixeira (1997). The iron-sulfur centers of the pyruvate:ferredoxin oxidoreductase from *Methanosarcina barkeri* (Fusaro). *FEBS Lett* **414**(2): 209-12.
- Boone, D. R., W. B. Whitman and P. Rouviere (1993). Diversity and Taxonomy of Methanogens. *Methanogenesis: Ecology, Physiology, Biochemistry and Genetics*. J. G. Ferry. New York, Chapman & Hall: 35-80.
- Bult, C. J., O. White, G. J. Olsen, L. Zhou, R. D. Fleischmann, G. G. Sutton, J. A. Blake, L. M. FitzGerald, R. A. Clayton, J. D. Gocayne, A. R. Kerlavage, B. A. Dougherty, J. F. Tomb, M. D. Adams, C. I. Reich, R. Overbeek, E. F. Kirkness, K. G. Weinstock, J. M. Merrick, A. Glodek, J. L. Scott, N. S. Geoghagen and J. C. Venter (1996). Complete genome sequence of the methanogenic archaeon, *Methanococcus jannaschii*. *Science* **273**(5278): 1058-73.
- Burggraf, S., A. Ching, K. O. Stetter and C. R. Woese (1991). The sequence of *Methanospirillum hungatei* 23S rRNA confirms the specific relationship between the extreme halophiles and the *Methanomicrobiales*. *Syst Appl Microbiol* **14**: 358-63.
- Charon, M. H., A. Volbeda, E. Chabriere, L. Pieulle and J. C. Fontecilla-Camps (1999). Structure and electron transfer mechanism of pyruvate:ferredoxin oxidoreductase. *Curr Opin Struct Biol* **9**(6): 663-9.
- Cytryn, E., D. Minz, R. S. Oremland and Y. Cohen (2000). Distribution and diversity of archaea corresponding to the limnological cycle of a hypersaline stratified lake (Solar lake, Sinai, Egypt). *Appl Environ Microbiol* **66**(8): 3269-76.

De Rosa, M., A. Gambacorta and A. Gliozzi (1986). Structure, biosynthesis, and physicochemical properties of archaebacterial lipids. *Microbiol Rev* **50**(1): 70-80.

Deppenmeier, U., A. Johann, T. Hartsch, R. Merkl, R. A. Schmitz, R. Martinez-Arias, A. Henne, A. Wiezer, S. Baumer, C. Jacobi, H. Bruggemann, T. Lienard, A. Christmann, M. Bomeke, S. Steckel, A. Bhattacharyya, A. Lykidis, R. Overbeek, H. P. Klenk, R. P. Gunsalus, H. J. Fritz and G. Gottschalk (2002). The genome of *Methanosarcina mazei*: evidence for lateral gene transfer between bacteria and archaea. *J Mol Microbiol Biotechnol* **4**(4): 453-61.

Devereux, R., S. H. He, C. L. Doyle, S. Orkland, D. A. Stahl, J. LeGall and W. B. Whitman (1990). Diversity and origin of *Desulfovibrio* species: phylogenetic definition of a family. *J Bacteriol* **172**(7): 3609-19.

DiMarco, A. A., K. A. Sment, J. Konisky and R. S. Wolfe (1990). The formylmethanofuran:tetrahydromethanopterin formyltransferase from *Methanobacterium thermoautotrophicum* delta H. Nucleotide sequence and functional expression of the cloned gene. *J Biol Chem* **265**(1): 472-6.

Docampo, R., S. N. Moreno and R. P. Mason (1987). Free radical intermediates in the reaction of pyruvate:ferredoxin oxidoreductase in *Tririchomonas foetus* hydrogenosomes. *J Biol Chem* **262**(26): 12417-20.

Eirich, L. D., G. D. Vogels and R. S. Wolfe (1978). Proposed structure for coenzyme F420 from *Methanobacterium*. *Biochemistry* **17**(22): 4583-93.

Ekiel, I., I. C. Smith and G. D. Sprott (1983). Biosynthetic pathways in *Methanospirillum hungatei* as determined by ¹³C nuclear magnetic resonance. *J Bacteriol* **156**(1): 316-26.

Ellefson, W. L. and R. S. Wolfe (1981). Component C of the methylreductase system of *Methanobacterium*. *J Biol Chem* **256**(9): 4259-62.

Ellermann, J., R. Hedderich, R. Bocher and R. K. Thauer (1988). The final step in methane formation. Investigations with highly purified methyl-CoM reductase (component C) from *Methanobacterium thermoautotrophicum* (strain Marburg). *Eur J Biochem* **172**(3): 669-77.

Ermler, U., W. Grabarse, S. Shima, M. Goubeaud and R. K. Thauer (1997). Crystal structure of methyl-coenzyme M reductase: the key enzyme of biological methane formation. *Science* **278**(5342): 1457-62.

Fauque, G., M. Teixeira, I. Moura, P. A. Lespinat, A. V. Xavier, D. V. Der Vartanian, H. D. Peck, Jr., J. Le Gall and J. G. Moura (1984). Purification, characterization and redox properties of hydrogenase from *Methanosarcina barkeri* (DSM 800). *Eur J Biochem* **142**(1): 21-8.

Ferry, J. G. (1999). Enzymology of one-carbon metabolism in methanogenic pathways. *FEMS Microbiol Rev* **23**(1): 13-38.

Fuchs, G., E. Stupperich and R. K. Thauer (1978). Acetate assimilation and the synthesis of alanine, aspartate and glutamate in *Methanobacterium thermoautotrophicum*. *Arch Microbiol* **117**(1): 61-6.

Fukuda, E. and T. Wakagi (2002). Substrate recognition by 2-oxoacid:ferredoxin oxidoreductase from *Sulfolobus* sp. strain 7. *Biochim Biophys Acta* **1597**(1): 74-80.

Galagan, J. E., C. Nusbaum, A. Roy, M. G. Endrizzi, P. Macdonald, W. FitzHugh, S. Calvo, R. Engels, S. Smirnov, D. Atnoor, A. Brown, N. Allen, J. Naylor, N. Stange-Thomann, K. DeArellano, R. Johnson, L. Linton, P. McEwan, K. McKernan, J. Talamas, A. Tirrell, W. Ye, A. Zimmer, R. D. Barber, I. Cann, D. E. Graham, D. A. Grahame, A. M. Guss, R. Hedderich, C. Ingram-Smith, H. C. Kuettner, J. A. Krzycki, J. A. Leigh, W. Li, J. Liu, B. Mukhopadhyay, J. N. Reeve, K. Smith, T. A. Springer, L. A. Umayam, O. White, R. H. White, E. Conway de Macario, J. G. Ferry, K. F. Jarrell, H. Jing, A. J. Macario, I. Paulsen, M. Pritchett, K. R. Sowers, R. V. Swanson, S. H. Zinder, E. Lander, W. W. Metcalf and B. Birren (2002). The genome of *M. acetivorans* reveals extensive metabolic and physiological diversity. *Genome Res* **12**(4): 532-42.

Gernhardt, P., O. Possot, M. Foglino, L. Sibold and A. Klein (1990). Construction of an integration vector for use in the archaebacterium *Methanococcus voltae* and expression of a eubacterial resistance gene. *Mol Gen Genet* **221**(2): 273-9.

Gloss, L. M. and R. P. Hausinger (1988). Methanogen factor 390 formation: species distribution, reversibility and effects of non-oxidative cellular stresses. *Biofactors* **1**(3): 237-40.

Goebel, B. M. and E. Stackebrandt (1994). Cultural and phylogenetic analysis of mixed microbial populations found in natural and commercial bioleaching environments. *Appl Environ Microbiol* **60**(5): 1614-21.

Graham, D. E., N. Kyrpides, I. J. Anderson, R. Overbeek and W. B. Whitman (2001). Genome of *Methanocaldococcus (Methanococcus) jannaschii*. *Methods Enzymol* **330**: 40-123.

Hawkins, C. F., A. Borges and R. N. Perham (1989). A common structural motif in thiamin pyrophosphate-binding enzymes. *FEBS Lett* **255**(1): 77-82.

Hedderich, R., A. Berkessel and R. K. Thauer (1990). Purification and properties of heterodisulfide reductase from *Methanobacterium thermoautotrophicum* (strain Marburg). *Eur J Biochem* **193**(1): 255-61.

Heider, J., X. Mai and M. W. Adams (1996). Characterization of 2-ketoisovalerate ferredoxin oxidoreductase, a new and reversible coenzyme A-dependent enzyme involved in peptide fermentation by hyperthermophilic archaea. *J Bacteriol* **178**(3): 780-7.

Jarrell, K. F. and S. F. Koval (1989). Ultrastructure and biochemistry of *Methanococcus voltae*. *Crit Rev Microbiol* **17**(1): 53-87.

Johnson, K. A. and D. E. Johnson (1995). Methane emissions from cattle. *J Anim Sci* **73**(8): 2483-92.

Jones, J. B., G. L. Dilworth and T. C. Stadtman (1979). Occurrence of selenocysteine in the selenium-dependent formate dehydrogenase of *Methanococcus vannielii*. *Arch Biochem Biophys* **195**(2): 255-60.

Jones, J. B. and T. C. Stadtman (1981). Selenium-dependent and selenium-independent formate dehydrogenases of *Methanococcus vannielii*. Separation of the two forms and characterization of the purified selenium-independent form. *J Biol Chem* **256**(2): 656-63.

Jones, W. J., Paynter M. J. B. and R. Gupta (1983). Characterization of *Methanococcus maripaludis* sp. nov., a new methanogen isolated from salt marsh sediment. *Arch Microbiol* **135**: 91-97.

Karrasch, M., G. Borner, M. Enssle and R. K. Thauer (1989). Formylmethanofuran dehydrogenase from methanogenic bacteria, a molybdoenzyme. *FEBS Lett* **253**(1-2): 226-30.

Keltjens, J. T. and C. van der Drift (1986). Electron transfer reactions in methanogens. *FEMS Microbiol Rev* **39**: 259-303.

Keltjens, J. T., G. C. Caerteling and G. D. Vogels (1986). Methanopterin and tetrahydromethanopterin derivatives: isolation, synthesis, and identification by high-performance liquid chromatography. *Methods Enzymol* **122**: 412-25.

Kengen, S. W., P. J. Daas, E. F. Duits, J. T. Keltjens, C. van der Drift and G. D. Vogels (1992). Isolation of a 5-hydroxybenzimidazolyl cobamide-containing enzyme involved in the methyltetrahydromethanopterin: coenzyme M methyltransferase reaction in *Methanobacterium thermoautotrophicum*. *Biochim Biophys Acta* **1118**(3): 249-60.

Kerscher, L. and D. Oesterhelt (1981). Purification and properties of two 2-oxoacid:ferredoxin oxidoreductases from *Halobacterium halobium*. *Eur J Biochem* **116**(3): 587-94.

- Kletzin, A. and M. W. Adams (1996). Molecular and phylogenetic characterization of pyruvate and 2-ketoisovalerate ferredoxin oxidoreductases from *Pyrococcus furiosus* and pyruvate ferredoxin oxidoreductase from *Thermotoga maritima*. *J Bacteriol* **178**(1): 248-57.
- Krampitz, L. O. (1969). Catalytic functions of thiamin diphosphate. *Annu Rev Biochem* **38**: 213-40.
- Lehmann-Richter, S., R. Grosskopf, W. Liesack, P. Frenzel and R. Conrad (1999). Methanogenic archaea and CO₂-dependent methanogenesis on washed rice roots. *Environ Microbiol* **1**(2): 159-66.
- Lester, R. L. and J. A. DeMoss (1971). Effects of molybdate and selenite on formate and nitrate metabolism in *Escherichia coli*. *J Bacteriol* **105**(3): 1006-14.
- Lin, Z. and R. Sparling (1998). Investigation of serine hydroxymethyltransferase in methanogens. *Can J Microbiol* **44**(7): 652-6.
- Lipman, D. J. and W. R. Pearson (1985). Rapid and sensitive protein similarity searches. *Science* **227**(4693): 1435-41.
- Ma, K. and R. K. Thauer (1990). Purification and properties of N₅, N₁₀-methylene tetrahydromethanopterin reductase from *Methanobacterium thermoautotrophicum* (strain Marburg). *Eur J Biochem* **191**(1): 187-93.
- Mai, X. and M. W. Adams (1994). Indolepyruvate ferredoxin oxidoreductase from the hyperthermophilic archaeon *Pyrococcus furiosus*. A new enzyme involved in peptide fermentation. *J Biol Chem* **269**(24): 16726-32.
- Mai, X. and M. W. Adams (1996). Characterization of a fourth type of 2-keto acid-oxidizing enzyme from a hyperthermophilic archaeon: 2-ketoglutarate ferredoxin oxidoreductase from *Thermococcus litoralis*. *J Bacteriol* **178**(20): 5890-6.
- Menon, A. L., H. Hendrix, A. Hutchins, M. F. Verhagen and M. W. Adams (1998). The delta-subunit of pyruvate ferredoxin oxidoreductase from *Pyrococcus furiosus* is a redox-active, iron-sulfur protein: evidence for an ancestral relationship with 8Fe-type ferredoxins. *Biochemistry* **37**(37): 12838-46.
- Mukhopadhyay, B., E. F. Johnson and R. S. Wolfe (1999). Reactor-scale cultivation of the hyperthermophilic methanarchaeon *Methanococcus jannaschii* to high cell densities. *Appl Environ Microbiol* **65**(11): 5059-65.
- Nolling, J. and J. N. Reeve (1997). Growth- and substrate-dependent transcription of the formate dehydrogenase (fdhCAB) operon in *Methanobacterium thermoformicum* Z-245. *J Bacteriol* **179**(3): 899-908.

- Ollivier, B., M. L. Fardeau, J. L. Cayol, M. Magot, B. K. Patel, G. Prensier and J. L. Garcia (1998). *Methanocalculus halotolerans* gen. nov., sp. nov., isolated from an oil-producing well. *Int J Syst Bacteriol* **48**: 821-8.
- Patel, G. B., J. H. E. Nash, B. J. Agnew and G. D. Sprott (1994). Natural and electroporation-mediated transformation of *Methanococcus voltae* protoplasts. *Appl Environ Microbiol* **60**: 907.
- Schauer, N. and J. G. Ferry (1982). Properties of Formate Dehydrogenase in *Methanobacterium formicum*. *J Bacteriol* **150**(1): 1-7.
- Schirch, L. V. and A. Diller (1971). Serine transhydroxymethylase. Affinity of the active site for substrates, substrate analogues, and anions. *J Biol Chem* **246**(12): 3961-6.
- Shieh, J. and W. B. Whitman (1988). Autotrophic acetyl coenzyme A biosynthesis in *Methanococcus maripaludis*. *J Bacteriol* **170**(7): 3072-9.
- Siddiqui, M. A., S. Fujiwara and T. Imanaka (1997). Indolepyruvate ferredoxin oxidoreductase from *Pyrococcus* sp. KOD1 possesses a mosaic structure showing features of various oxidoreductases. *Mol Gen Genet* **254**(4): 433-9.
- Skidmore, M. L., J. M. Foght and M. J. Sharp (2000). Microbial life beneath a high arctic glacier. *Appl Environ Microbiol* **66**(8): 3214-20.
- Slesarev, A. I., K. V. Mezhevaya, K. S. Makarova, N. N. Polushin, O. V. Shcherbinina, V. V. Shakhova, G. I. Belova, L. Aravind, D. A. Natale, I. B. Rogozin, R. L. Tatusov, Y. I. Wolf, K. O. Stetter, A. G. Malykh, E. V. Koonin and S. A. Kozyavkin (2002). The complete genome of hyperthermophile *Methanopyrus kandleri* AV19 and monophyly of archaeal methanogens. *Proc Natl Acad Sci U S A* **99**(7): 4644-9.
- Smith, D. R., L. A. Doucette-Stamm, C. Deloughery, H. Lee, J. Dubois, T. Aldredge, R. Bashirzadeh, D. Blakely, R. Cook, K. Gilbert, D. Harrison, L. Hoang, P. Keagle, W. Lumm, B. Pothier, D. Qiu, R. Spadafora, R. Vicaire, Y. Wang, J. Wierzbowski, R. Gibson, N. Jiwani, A. Caruso, D. Bush, J. N. Reeve and et al. (1997). Complete genome sequence of *Methanobacterium thermoautotrophicum* deltaH: functional analysis and comparative genomics. *J Bacteriol* **179**(22): 7135-55.
- Sparling, R. and L. Daniels (1990). Regulation of formate dehydrogenase activity in *Methanococcus thermolithotrophicus*. *J Bacteriol* **172**(3): 1464-9.
- Tersteegen, A., D. Linder, R. K. Thauer and R. Hedderich (1997). Structures and functions of four anabolic 2-oxoacid oxidoreductases in *Methanobacterium thermoautotrophicum*. *Eur J Biochem* **244**(3): 862-8.
- Thauer, R. K., K. Jungermann and K. Decker (1977). Energy conservation in chemotrophic anaerobic bacteria. *Bacteriol Rev* **41**(1): 100-80.

- Tumbula, D. L., R. A. Makula and W. B. Whitman (1994). Transformation of *Methanococcus maripaludis* and identification of a PstI-like restriction system. FEMS Microbiol Lett **121**: 309-314.
- Tumbula, D. L., T. L. Bowen and W. B. Whitman (1997). Characterization of pURB500 from the archaeon *Methanococcus maripaludis* and construction of a shuttle vector. J Bacteriol **179**(9): 2976-86.
- Tumbula, D. L. and W. B. Whitman (1999). Genetics of *Methanococcus*: possibilities for functional genomics in Archaea. Mol Microbiol **33**(1): 1-7.
- Uyeda, K. and J. C. Rabinowitz (1971). Pyruvate-ferredoxin oxidoreductase. IV. Studies on the reaction mechanism. J Biol Chem **246**(10): 3120-5.
- Vermeij, P., E. Vinke, J. T. Keltjens and C. Van der Drift (1995). Purification and properties of coenzyme F390 hydrolase from *Methanobacterium thermoautotrophicum* (strain Marburg). Eur J Biochem **234**(2): 592-7.
- Wasserfallen, A., J. Nolling, P. Pfister, J. Reeve and E. Conway de Macario (2000). Phylogenetic analysis of 18 thermophilic *Methanobacterium* isolates supports the proposals to create a new genus, Methanothermobacter gen. nov., and to reclassify several isolates in three species, *Methanothermobacter thermoautotrophicus* comb. nov., *Methanothermobacter wolfeii* comb. nov., and *Methanothermobacter marburgensis* sp. nov. Int J Syst Evol Microbiol **50**: 43-53.
- White (2000). The Physiology and Biochemistry of Prokaryotes. New York, Oxford University Press.
- Whitford, M. F., R. M. Teather and R. J. Forster (2001). Phylogenetic analysis of methanogens from the bovine rumen. BMC Microbiol **1**(1): 5.
- Whitman, W. B., Shieh, J., Sohn, S., Caras, D. S. and U. Premachandran (1986). Isolation and characterization of 22 mesophilic methanococci. System Appl Microbiol. **7**: 235-240.
- Woese, C. R., O. Kandler and M. L. Wheelis (1990). Towards a natural system of organisms: proposal for the domains Archaea, Bacteria, and Eucarya. Proc Natl Acad Sci U S A **87**(12): 4576-9.
- Wood, A. G., W. B. Whitman and J. Konisky (1989). Isolation and characterization of an archaeobacterial viruslike particle from *Methanococcus voltae* A3. J Bacteriol **171**(1): 93-8.
- Xing, R. Y. and W. B. Whitman (1987). Sulfometuron methyl-sensitive and -resistant acetolactate synthases of the archaeobacteria *Methanococcus* spp. J Bacteriol **169**(10): 4486-92.

Xing, R. Y. and W. B. Whitman (1991). Characterization of enzymes of the branched-chain amino acid biosynthetic pathway in *Methanococcus* spp. *J Bacteriol* **173**(6): 2086-92.

Xing, R. Y. and W. B. Whitman (1992). Characterization of amino acid aminotransferases of *Methanococcus aeolicus*. *J Bacteriol* **174**(2): 541-8.

Xing, R. and W. B. Whitman (1994). Purification and characterization of the oxygen-sensitive acetohydroxy acid synthase from the archaeobacterium *Methanococcus aeolicus*. *J Bacteriol* **176**(5): 1207-13.

Zellner, G., E. Stackebrandt, P. Messner, B. J. Tindall, E. Conway de Macario, H. Kneifel, U. B. Sleytr and J. Winter (1989). *Methanocorpusculaceae* fam. nov., represented by *Methanocorpusculum parvum*, *Methanocorpusculum sinense* spec. nov. and *Methanocorpusculum bavaricum* spec. nov. *Arch Microbiol* **151**(5): 381-90.

Zhang, Q., T. Iwasaki, T. Wakagi and T. Oshima (1996). 2-oxoacid:ferredoxin oxidoreductase from the thermoacidophilic archaeon, *Sulfolobus* sp. strain 7. *J Biochem (Tokyo)* **120**(3): 587-99.